SUPPLEMENTARY INFORMATION

Supplementary Tables

S1: Table of plasmid/constructs

Construct Name	Promoter	Gene	Mammalian Selection	Role in this work
pEV-UAS-H2B-citrine	UAS	H2B-citrine	Zeocin	Reporter for hN1-Gal4^{esn}
pEV-12xCSL-H2B-citrine	12xCSL	H2B-citrine	Zeocin	Reporter for hN1
pcDNA3-hN1-mod1	CMV	hNotch1	Neomycin	hN1 construct
pcDNA3-hN1-mcherry	CMV	hN1-mcherry	Neomycin	hN1 construct (used)
pCDNA3-hNECD – Gal4^{esn}	CMV	hNECD – Gal4^{esn}	Neomycin	hN1-Gal4^{esn} construct
pcDNA5/TO-hNICD-Gal4^{esn}	CMV-TO	hNICD-Gal4^{esn}	Hygromycin	hNICD-Gal4^{esn}
pcDNA5/TO-Delta-mcherry	CMV-TO	Delta-mcherry	Hygromycin	Inducible Delta-mCherry
pcDNA5/TO-Gal4^{esn}	CMV-TO	Gal4^{esn}	Hygromycin	Inducible Gal4^{esn}
pCS-H2B-cerulean	CMV	H2B-cerulean	-	Segmentation color
pcDNA6-UAS-H2B-citrine	UAS	H2B-citrine	Blasticidin	Reporter in dual reporter line
pEV-12xCSL-H2B-mcherry	12xCSL	H2B-mcherry	Zeocin	Reporter in dual reporter line

S2: Table of stable cell lines

Stable Cell Line	Parental Line	Transfected Construct	Antibiotic Selection
T-REx-CHO-K1 (Invitrogen)	-	-	Blasticidin (10 ug/ml)
12xCSL-H2B-Citrine	T-REx-CHO-K1	pEV-12xCSL-H2B-Citrine	Zeocin (400 ug/ml), Blasticidin (10 ug/ml)
UAS-H2B-Citrine + CMV-H2B-Cerulean	T-REx-CHO-K1	pEV-UAS-H2B-Citrine pCS-H2B-Cerulean	Zeocin (400 ug/ml), Blasticidin (10 ug/ml)
hN1-No-Delta	12xCSL-H2B-Citrine	pcDNA3-hN1-mCherry	Zeocin (400 ug/ml), Blasticidin (10 ug/ml), Geneticin (600 ug/ml)
hN1G4^{esn}-No-Delta	UAS-H2B-Citrine + CMV-Cerulean	pcDNA3-hNECD-Gal4^{esn}	Zeocin (400 ug/ml), Blasticidin (10 ug/ml), Geneticin (600 ug/ml)
hN1	hN1-No-Delta	pcDNA5-TO-Dl-mCherry pCS-H2B-Cerulean	Zeocin (400 ug/ml), Blasticidin (10 ug/ml), Geneticin (600 ug/ml), Hygromycin (500 ug/ml)
hN1G4^{esn}	hN1G4^{esn}-No-Delta	pcDNA5-TO-Dl-mCherry	Zeocin (400 ug/ml), Blasticidin (10 ug/ml), Geneticin (600 ug/ml), Hygromycin (500 ug/ml)
TO-DMC	T-REx-CHO-K1	pcDNA5-TO-Dl-mCherry	Hygromycin (500 ug/ml), Blasticidin (10 ug/ml)
TO-DMC+hN1G4^{esn} (for fig. S9)	TO-DMC	pcDNA3-hNECD-Gal4^{esn}	Hygromycin (500 ug/ml), Blasticidin (10 ug/ml), Geneticin (600 ug/ml)
TO-Gal4^{esn}	UAS-H2B-Citrine + CMV-H2B-Cerulean	pcDNA5/TO-Gal4^{esn}	Zeocin (400 ug/ml), Blasticidin (10 ug/ml), Hygromycin (500 ug/ml)
UAS-H2B-Citrine	CHO-K1 (CCL-61)	pcDNA-UAS-H2B-Citrine	Blasticidin (10 ug/ml)
UAS-H2B-Citrine + 12xCSL-H2B-mCherry (dual reporter)	UAS-H2B-Citrine	pEV-12xCSL-H2B-Citrine	Zeocin (400 ug/ml), Blasticidin (10ug/ml)

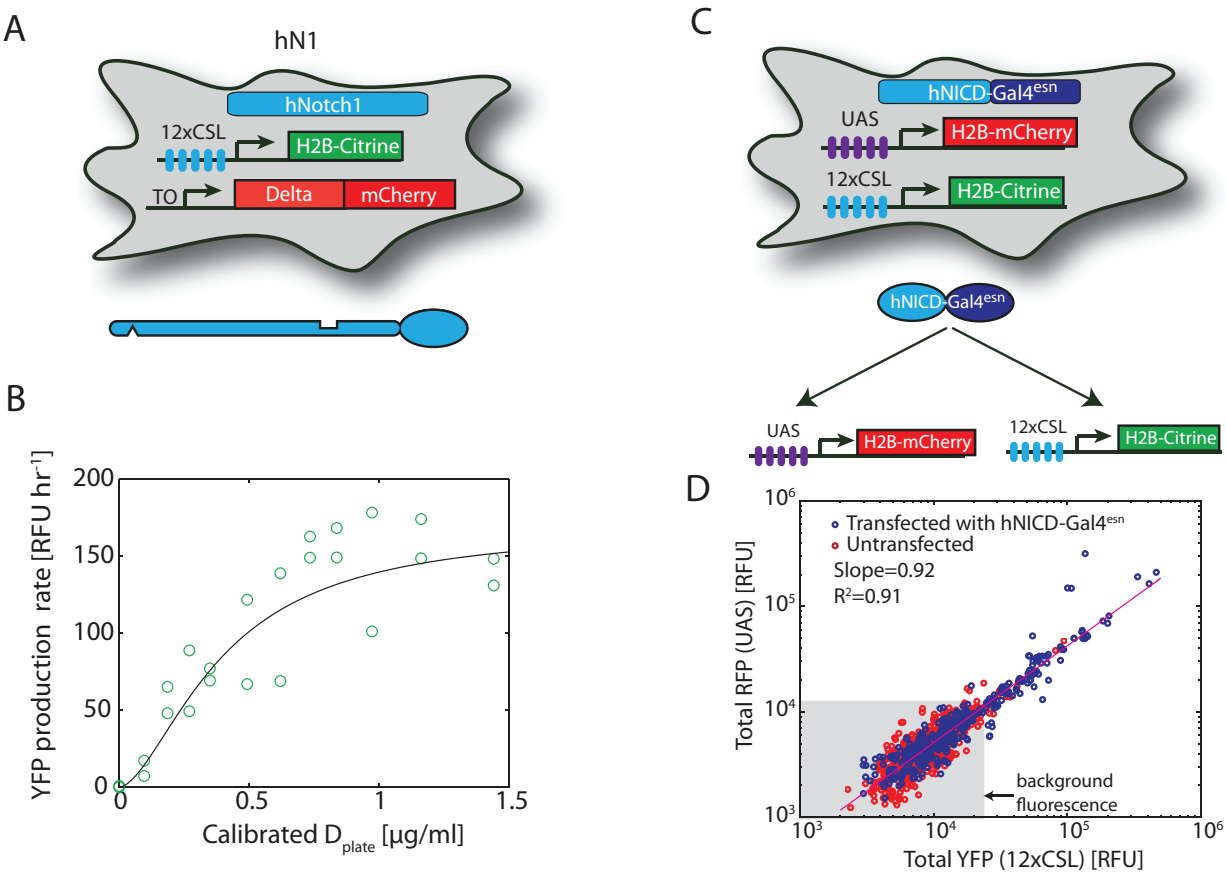

Figure S1: hN1G4^{esn} and hN1 cell lines exhibit similar response. (A) The hN1 cell line stably incorporates genes for full length hNotch1, Histone 2B (H2B)-Citrine (YFP) reporter controlled by a synthetic 12XCSL promoter[30], and a Tet-inducible Delta-mCherry fusion protein. It also constitutively express H2B-Cerulean (CFP) for image segmentation (not shown). Note that the hN1 cell line includes an mCherry domain fused to the C-terminus of hNotch1, which is not detectable experimentally and therefore omitted in the diagram. These cells exhibit no detectable endogenous Notch or Delta activities. (B) Notch response to trans-Delta in the hN1 cell line is similar to the one in hN1G4^{esn} (Fig. 2). Hill coefficient n=1.6 (95% CI: 0.6-2.5). (C-D) Co-linear response of the 12xCSL and the UAS promoters. (C) A fusion protein consisting of Gal4^{esn} and the Notch Intracellular Domain (ICD) was transiently transfected into a CHO-K1 cell line containing two stably integrated reporters: 12xCSL-H2B-Citrine and UAS-H2B-mCherry. (C) Total RFP fluorescence versus total YFP fluorescence for transfected (blue circles) or untransfected (red circles) cells shows a co-linear response of the two reporters to the fusion activator (plotted on a log-log scale). A linear regression fit shows a slope of 0.92 (R^2=0.91), corresponding to a nearly linear relation between the two reporters (red line). Background fluorescence (gray area) is due to basal leakiness of reporters. Note that, due to the finite transfection efficiency of the transient transfection, only some of the cells contain the fusion activator. Data points are extracted from fluorescence images of cells, and analyzed using the techniques described in the text and methods. This result together with the non-cooperative behavior of the Gal^{esn}-UAS system shown in Fig. S2 is consistent with a non-cooperative activation of the 12xCSL promoter by Notch ICD.

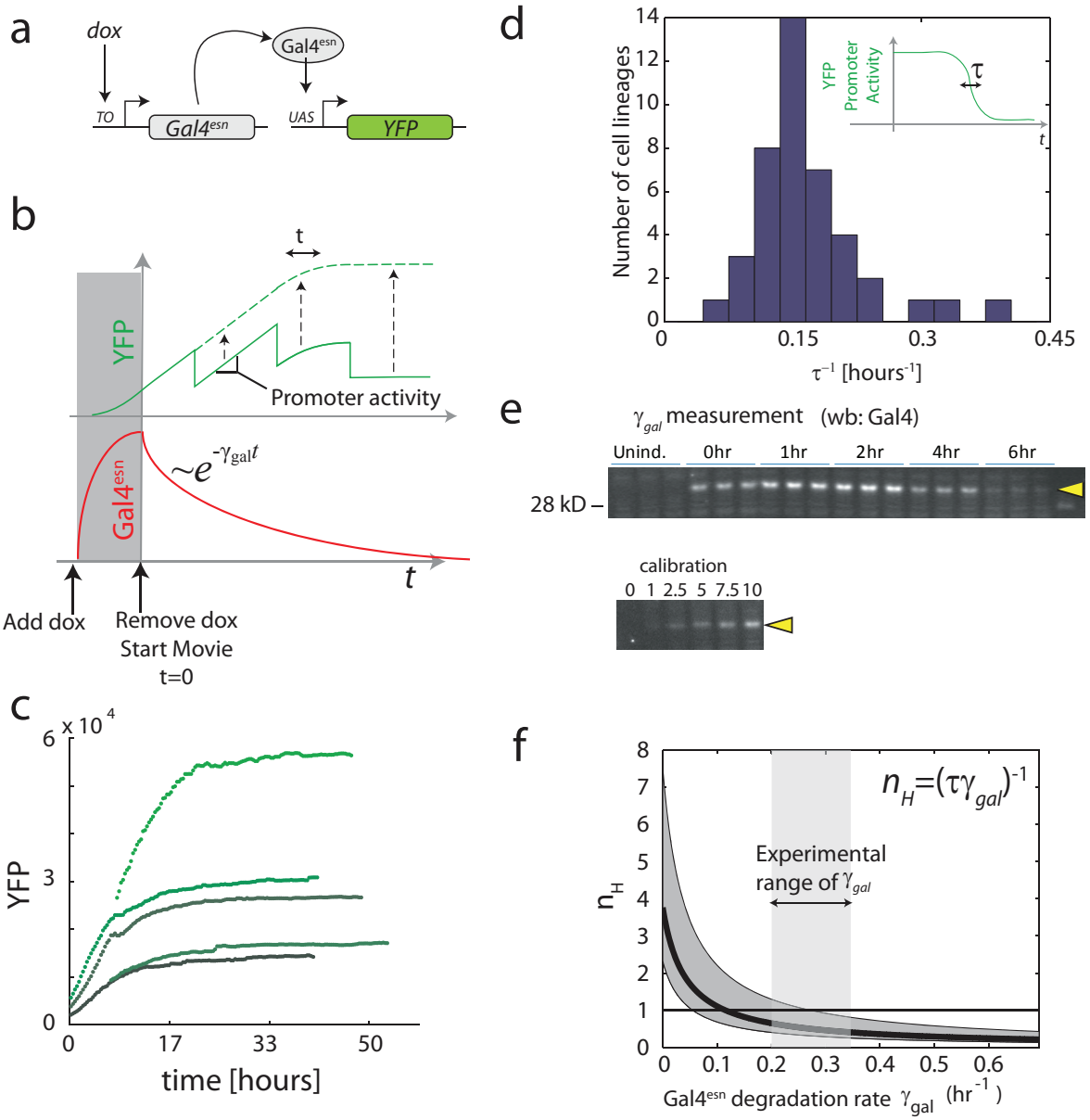

Figure S2: The Gal4^{esn}-UAS transcription factor-promoter interaction shows no cooperativity. This figure describes a measurement of the relationship between Gal4^{esn} concentration and the transcriptional activity of its target UAS promoter. As in Fig. 3A and ref. 2, the approach involves allowing the transcription factor to decay and/or dilute while following the activity of its target promoter. (a) Schematic of cell line design. In this cell line, Gal4^{esn} is expressed from a *tet*-dependent promoter under the control of the doxycyline inducer. Gal4^{esn} activates expression of an H2B-YFP (Citrine) reporter gene. (b) Schematic of experimental design. Prior to the start of the movie, cells were induced with a pulse of doxycycline, which was then washed out immediately before the beginning of time-lapse movie recording. Consequently, Gal4^{esn} was expressed, and then allowed to degrade and/or dilute over time (red curve, bottom panel), while H2B-YFP fluorescence was monitored in individual cell lineages (top panel). γ_{gal} denotes the effective decay rate of Gal4^{esn}. For large enough pulses of Gal4^{esn} expression, the resulting data (shown schematically) would be expected to show constant rates of production of YFP (slopes of green line), interrupted by a ~2-fold decrease in YFP levels at cell division events, due to partitioning of the YFP to daughter cells. To avoid discontinuities inherent to cell division events, the "lost" fluorescence after division is replaced (computationally) after each cell division event (dashed line and arrows). The slope of the resulting (dashed) trace is directly related to the activity of the UAS promoter, shown in the inset of (d). Here we focus on τ, the relative timescale required for the

slope to fall from 73% to 23% of its initial value as Gal4^{esn} decays (cf. Fig. 3A). (c) Observed YFP accumulation in individual cell lineages. These traces have been corrected for cell division events as shown in (b). (d) Histogram of measured τ values determined from traces like those in (c) shows that, despite variability in initial levels of expression, the timescales, τ, required for turn off were relatively constant. (e) Using a time-course Western blot against Gal4^{esn}, we observed the Gal4^{esn} half-life to be between ~3-5 hours (i.e. $\gamma_{gal} \sim 0.2 - 0.33$). A calibration with varying levels of cell lysate was also run to test linearity of measurement (bottom). (f) Inferring the Hill coefficient of the Gal4^{esn}-UAS interaction based on the measured values of τ and γ_{gal}, using the relationship shown in equation, inset. The black line shows how measurements of γ_{gal} constrain the possible range of underlying Hill coefficients. The dark gray region indicates the range of n_H values consistent with variability in the measurement of τ in (f). The light gray region indicates the measured range of γ_{gal}. The intersection between the two gray regions provide the range of likely for n_H values. This result shows that the effective cooperativity of the Gal4^{esn}-UAS interaction does not significantly exceed 1.

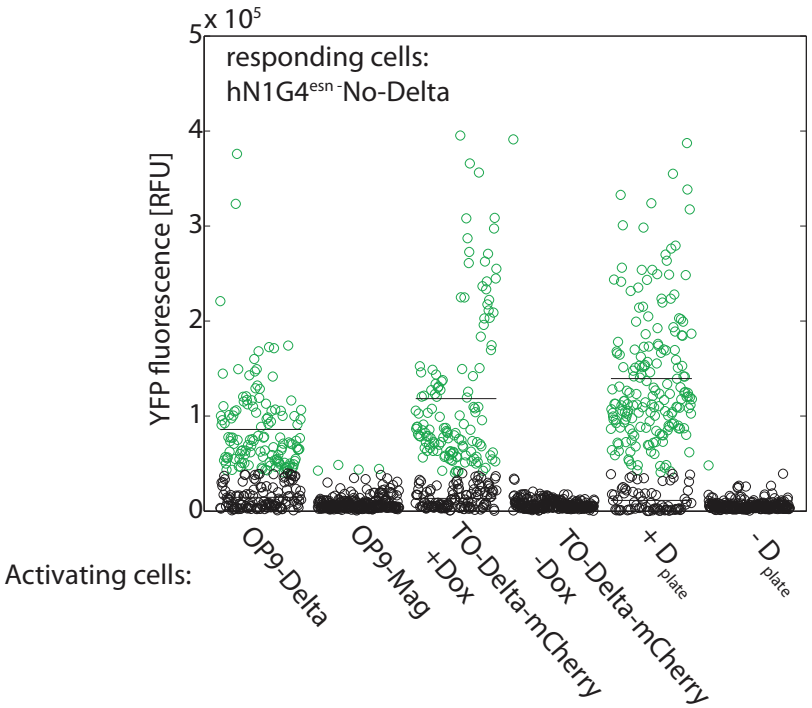

Figure S3: TO-Delta-mCherry cells trans-activate as efficiently as OP9-Delta cells. We compared the relative abilities of the TO-Delta-mCherry cell line, the OP9-Delta cell line, and D_{plate} to trans-activate Notch. Stromal OP9 cells stably expressing mDll1 (OP9-Delta) and control OP9 cells not expressing Delta[1] (both are a generous gift from Ellen Rothenberg) and inducible CHO TO-Delta-mCherry cells were co-cultured with hN1G4^{esn}-No-Delta cells (containing Notch and a reporter only—see Fig. S5). Cells were plated at a ratio of (70% Delta cells :30% Notch cells) at cell density of 1x10^5 cells/ml and incubated for 48 hours, and then imaged in an epifluorescence microscope. TO-Delta-mCherry cells were either induced with 100ng/ml Dox or not induced, as indicated. A set of controls with Notch reporter cells grown with or without plate-bound Delta (indicated by $+D_{plate}$ and $-D_{plate}$, respectively) were measured at the same time. Green and Black circles correspond to YFP fluorescence of activated and non-activated Notch cells, respectively (n=259 cells in each sample).

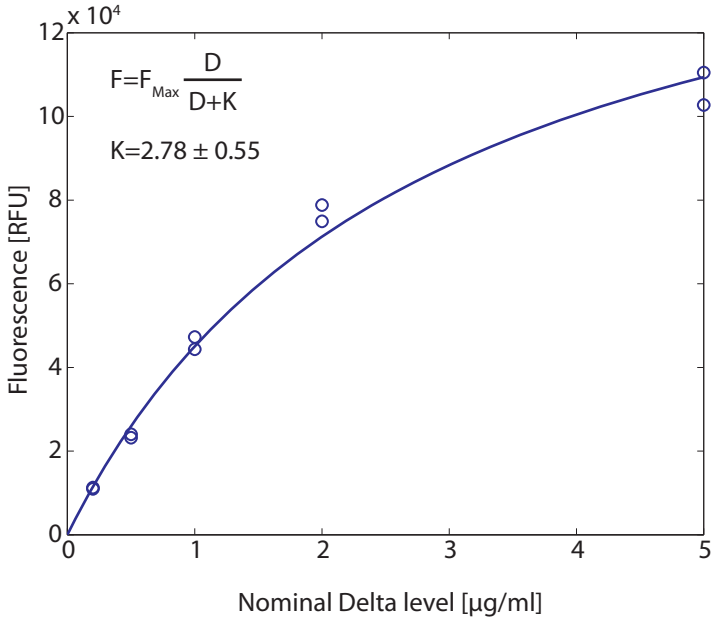

Figure S4: Calibration of plate bound Delta. Plates were incubated with different concentrations of IgG-Delta^{ext} (see methods for complete protocol). We determined the relationship between the concentration of IgG-Delta^{ext} used during incubation and the amount of IgG-Delta^{ext} actually adsorbed to the plate using a fluorescence binding assay. Right after incubation, plates were treated with anti-human-IgG conjugated to Alexa488 (Invitrogen). Fluorescence levels were measured using a plate reader (Wallac 1420, Perkin-Elmer). As seen in the figure, the binding of IgG-Delta^{ext} starts to saturate at concentrations bigger than 2ug/ml and is well-fit by the Michaelis-Menten curve $D_{plate} = \frac{D_{nominal}}{1+D_{nominal}/K}$, with $K = 2.78$ and where $D_{nominal}$ is the concentration of IgG-Delta^{ext} used in the incubation step. In addition, to assess the spatial uniformity of D_{plate}, we took snapshots of the bound antibody using a fluorescence microscope (not shown). We estimate the plate-plate variation in D_{plate} at 10-20%.

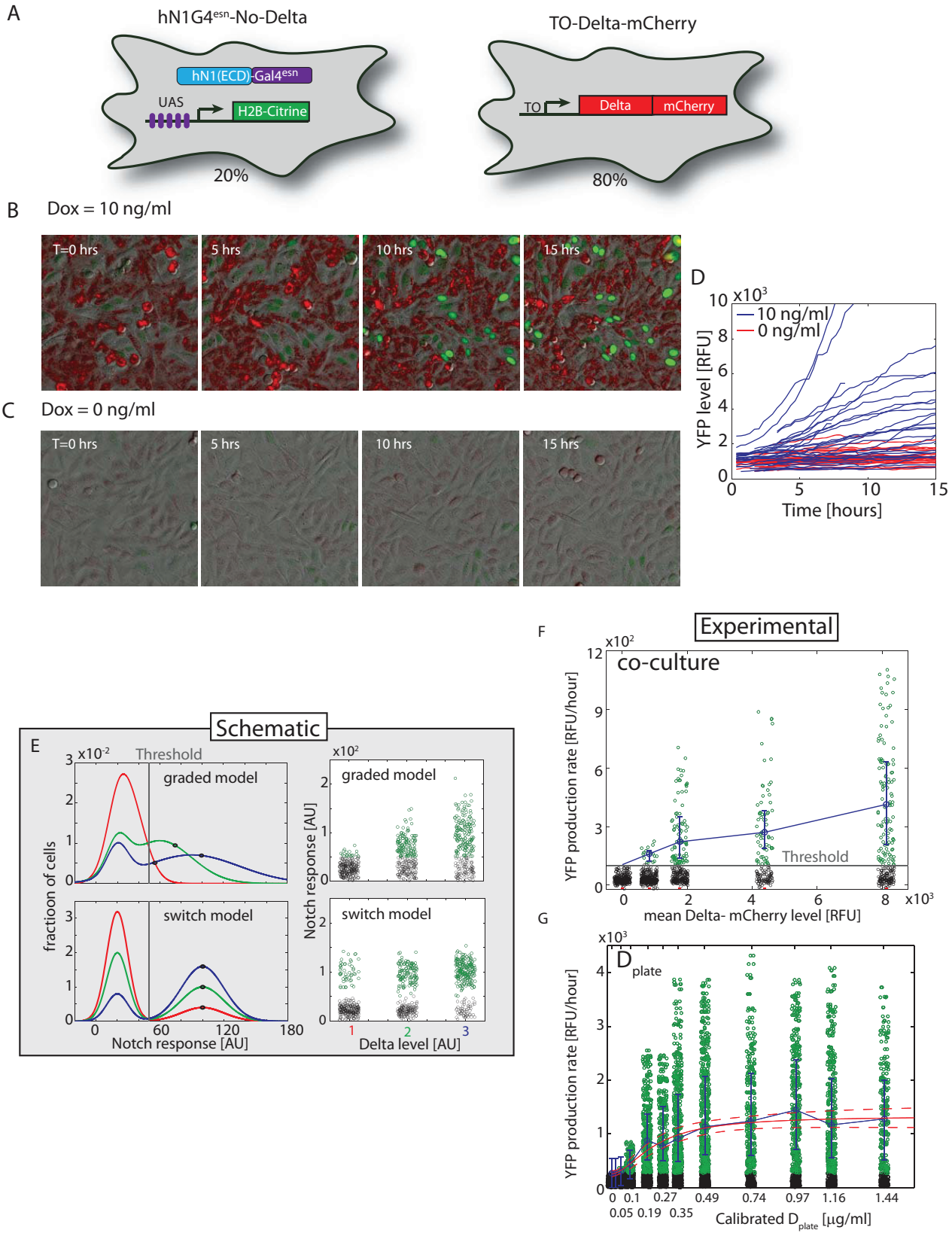

Figure S5: Notch activity responds to trans-activation by cell-bound Delta in a graded fashion. (A) In order to analyze trans-activation between cells, we co-cultured two cell lines, one expressing hN1G4^{esn} and a reporter (hN1G4^{esn}-No-Delta cell line, left), and one containing only inducible Delta-mCherry (TO-DMC cell line, right). See Table S2 for strain descriptions. (B) Filmstrip of intercellular trans-activation

taken from Movie S3. Here, the hN1G4^{esn}-No-Delta cell line (green nuclei) was co-cultured with TO-DMC cell line induced with 10ng/ml doxycycline to express Delta-mCherry (red cytoplasmic staining). Cell lines were co-cultured at a density ratio of 80:20 (TO-DMC: hN1G4^{esn}–No-Delta). Note the increasing Notch reporter fluorescence over time. (C) In contrast, without induction (no doxycycline), we observed much lower activation of Delta-mCherry expression and Notch activity in the reporter cell lines. Note that color (intensity) scales in (B) and (C) are the same. (D) Single cell tracks from the two movies shown in B and C. (E) Distinguishing between two possible models of activation in this experiment: graded and switch-like (schematic). Both models assume that some fraction of the cells do not respond even at maximal activation (here, we assume 20% 'non responders'). In the graded model, the responding population shows an increase of its median (black circles) response above a threshold, with higher induction levels (coefficient of variation is kept fixed). In the switch-like model, cells are in either the 'on' or 'off' states; only the fraction of cells occupying the 'on' state increases with Delta. Note that the two models predict qualitatively different responses of the mean number of activated cells with increasing Delta. (F) Experimental analysis of Notch reporter activation in individual cells (YFP production rates) at different levels of mean Delta-mCherry induction. The green circles correspond to single cell YFP production rates in the hN1G4^{esn}-No-Delta cell line above the threshold, determined by the basal expression without any Delta-mCherry induction in the TO-DMC cell line (a). The black circles correspond to cells that do not respond or that respond at levels below the threshold. The blue circles correspond to the median of activated cells. Error bars denote the 25 and 75 percentiles of the activated cells distributions. The response is consistent with a graded, rather than switch-like, model of trans-activation (e). (G) For comparison, a similar analysis was performed on the plate-bound Delta induction data shown in Fig. 2 c,d. Here, individual data points correspond to rates of YFP production. Note the graded, saturating response of the median response (blue data points and line) to D_{plate}. The red lines indicate a best fit of these median responses to a Hill function, with 95% confidence intervals bounded by the dashed red lines. The best fit Hill coefficient was 1.8 ± 0.9, in agreement with values obtained in Fig. 2D. Note that the relative fluorescence unit (RFU) scales in (F) and (G) are different due to the use of different imaging conditions. Together, these results show, first, that plate-bound and cell-expressed Delta trans-activate with similar cooperativity, and second, that the analysis based on population average response shown in Fig. 2D for plate-bound Delta produces equivalent results to the single-cell analysis of activation by cellular Delta.

A

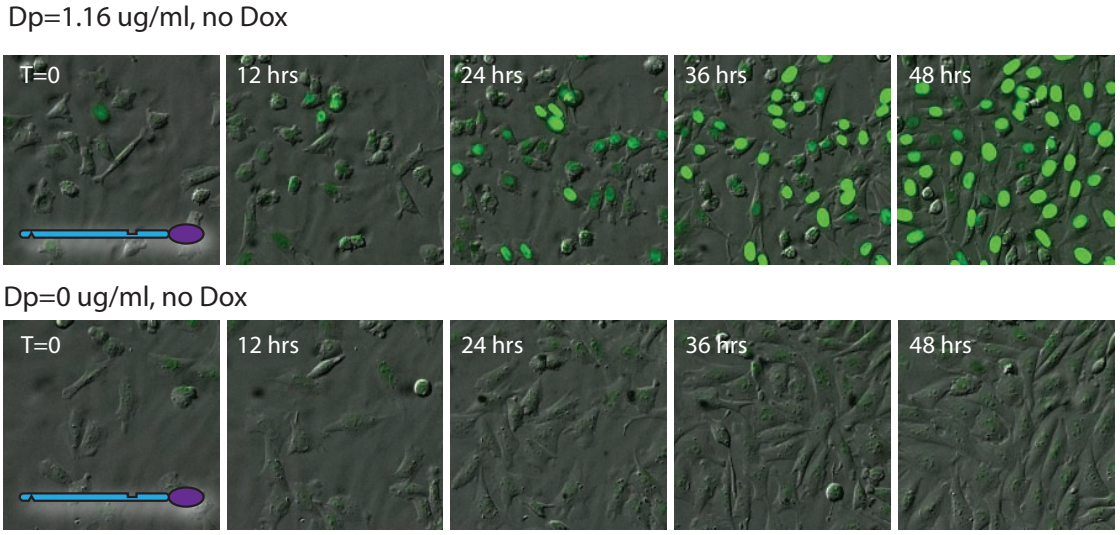

B

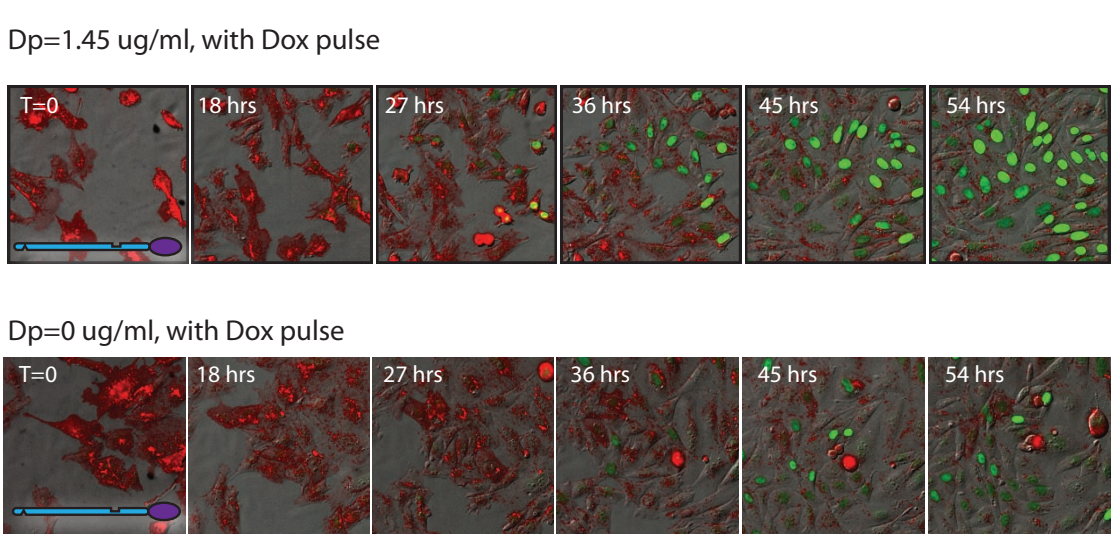

Figure S6: Induction at D_{plate}=0 is small compared to higher D_{plate} levels. (A) Filmstrips comparing activation of hN1G4^{esn} cells at D_{plate}=0 and D_{plate}=1.16 µg/ml (Fig. 2B). No induction is observed at D_{plate}=0. (B) Filmstrips comparing activation of hN1G4^{esn} cells induced with a doxycycline pulse at D_{plate}=0 and D_{plate}=1.16ug/ml (Fig. 2B). Only very few cells are induced in this case compared to higher D_{plate}. Thus, at this cell density transactivation between hN1G4^{esn} cells has only a small effect (this is also seen in the average data in Fig. 3G).

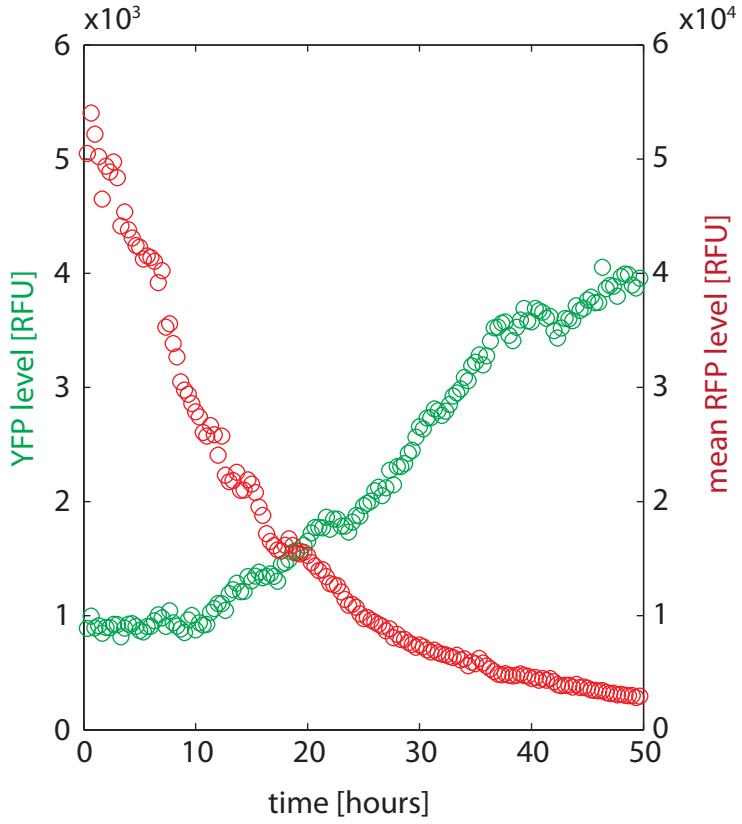

Figure S7: The hN1 cell line also shows an ultrasensitive response. hN1 cells show delayed turn-on in Notch signaling in response to slow decay of Delta-mCherry. Protocol is as described in Fig. 3A.

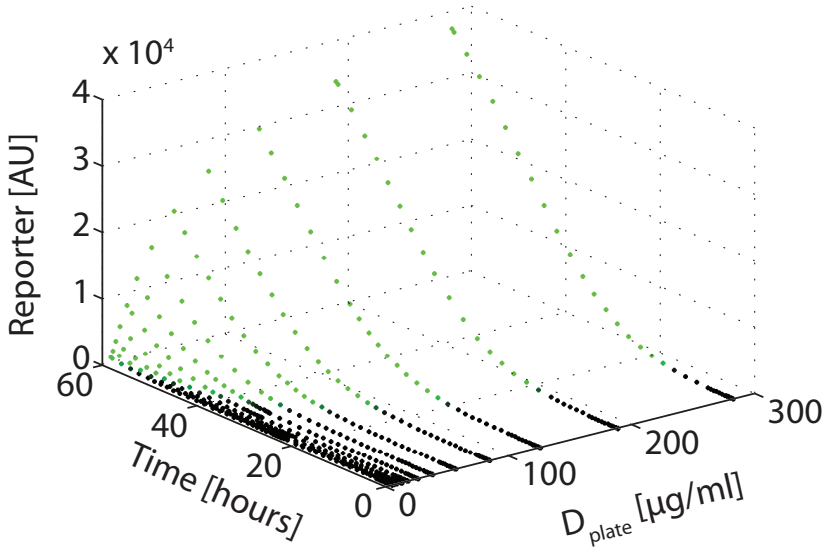

Figure S8: Delta inactivation by Notch is required for sharp responses to cis-Delta at fixed threshold. We simulated a model in which Delta inactivates Notch catalytically. In this model Delta is assumed to be recycled back after interaction with Notch (See theoretical supplementary for derivation and parameters). Note that, unlike the simulations based on the mutual inactivation model (Fig. 3H), here the turn-on curves do not exhibit sharp responses, and the threshold positions vary with D_{plate}. Note that the range of D_{plate} was scaled up to show the full response spectrum because a much higher D_{plate} is required to overcome the effect of D_{cis}.

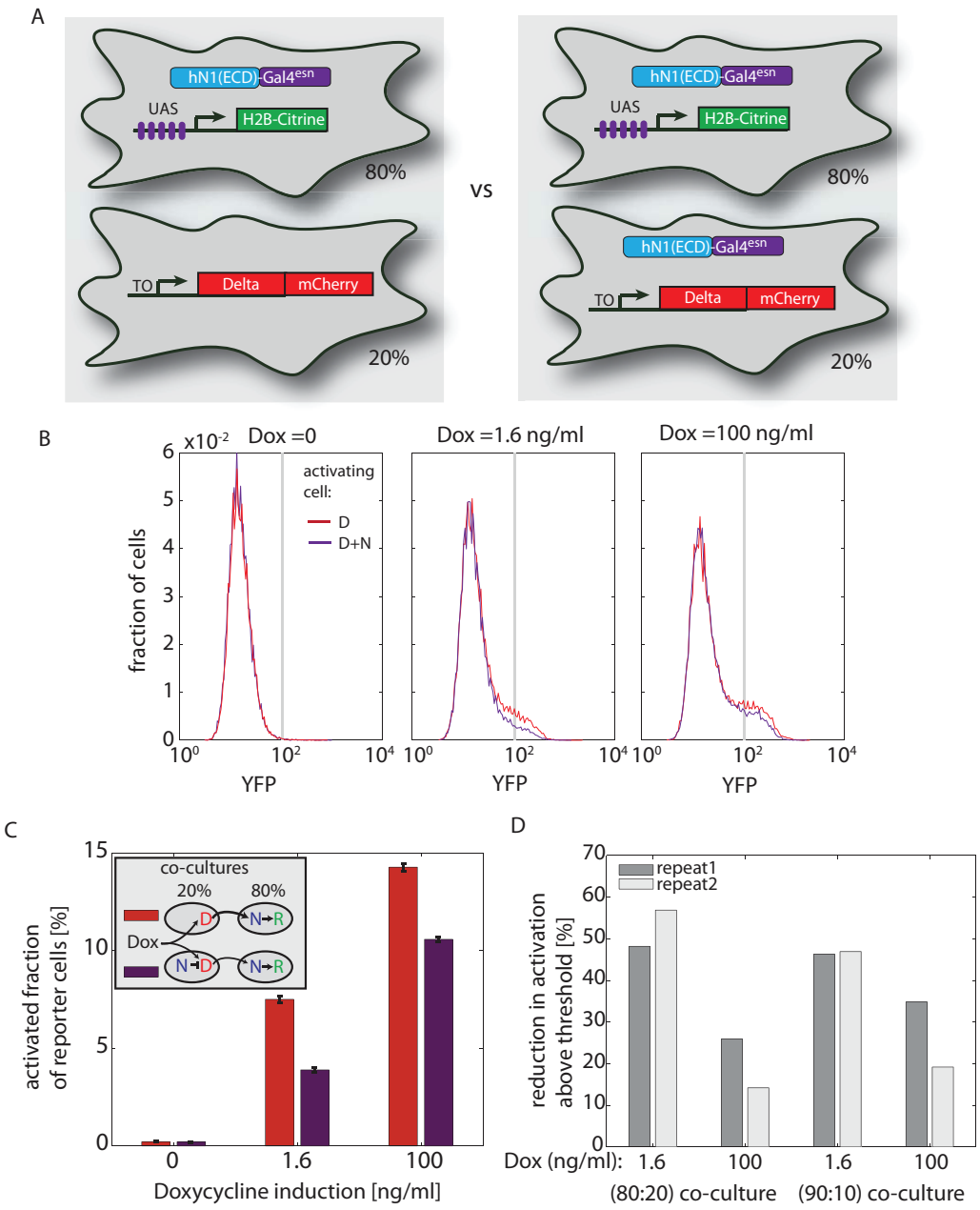

Figure S9: Notch cis-inactivates Delta. (A) Cells expressing hN1G4^{esn} and a UAS-H2B-Citrine reporter (hN1G4^{esn}–No-Delta) were cocultured with cells expressing Delta (TO-DMC) or cells expressing Notch and Delta (TO-Delta-mCherry+hN1G4^{esn}). Note that TO-Delta-mCherry+hN1G4^{esn} cell line does not contain a reporter. This enables measurement of the response only from the Notch reporter cells. The level of Delta-mCherry in both of the inducing cell lines is similar across a wide dox induction range (not shown) providing evidence that Notch does not induce Delta degradation. Experimental procedure: Cells were co-cultured at the indicated ratios and plated at 1x10^5 cells/ml. Cells were subjected to a 12 hour doxycycline pulse (weak induction) with different dox levels. FACS analysis was performed 24 hours after the dox pulse using a FACSCalibur. (B) Fluorescence distributions in co-culture experiments. A total of 50,000 cells were measured for each sample. Only cells containing the Notch reporter are shown. The activation threshold (gray vertical line) is defined as a fluorescence level greater than that of 99.5% of negative control (dox=0). (C) Fraction of cells above threshold for the co-culture experiments shown in (B). Standard errors were estimated using a bootstrapping method by calculating the standard error of 20 non-overlapping subsamples. Note that the difference in the fraction of activated cells between the two samples is largest at intermediate Delta induction. This is consistent with the mutual inactivation model since the titration level of Notch should have larger effect at lower Delta expressions. (D) Qualitatively similar results were obtained in a repeat performed on a different day (dark gray vs light gray). Furthermore the relative reduction in activation of cells between the two samples remains similar even when the relative fractions of the two cell lines are changed to 10% Delta (or Delta+ Notch) cells and 90% Notch reporter cells.

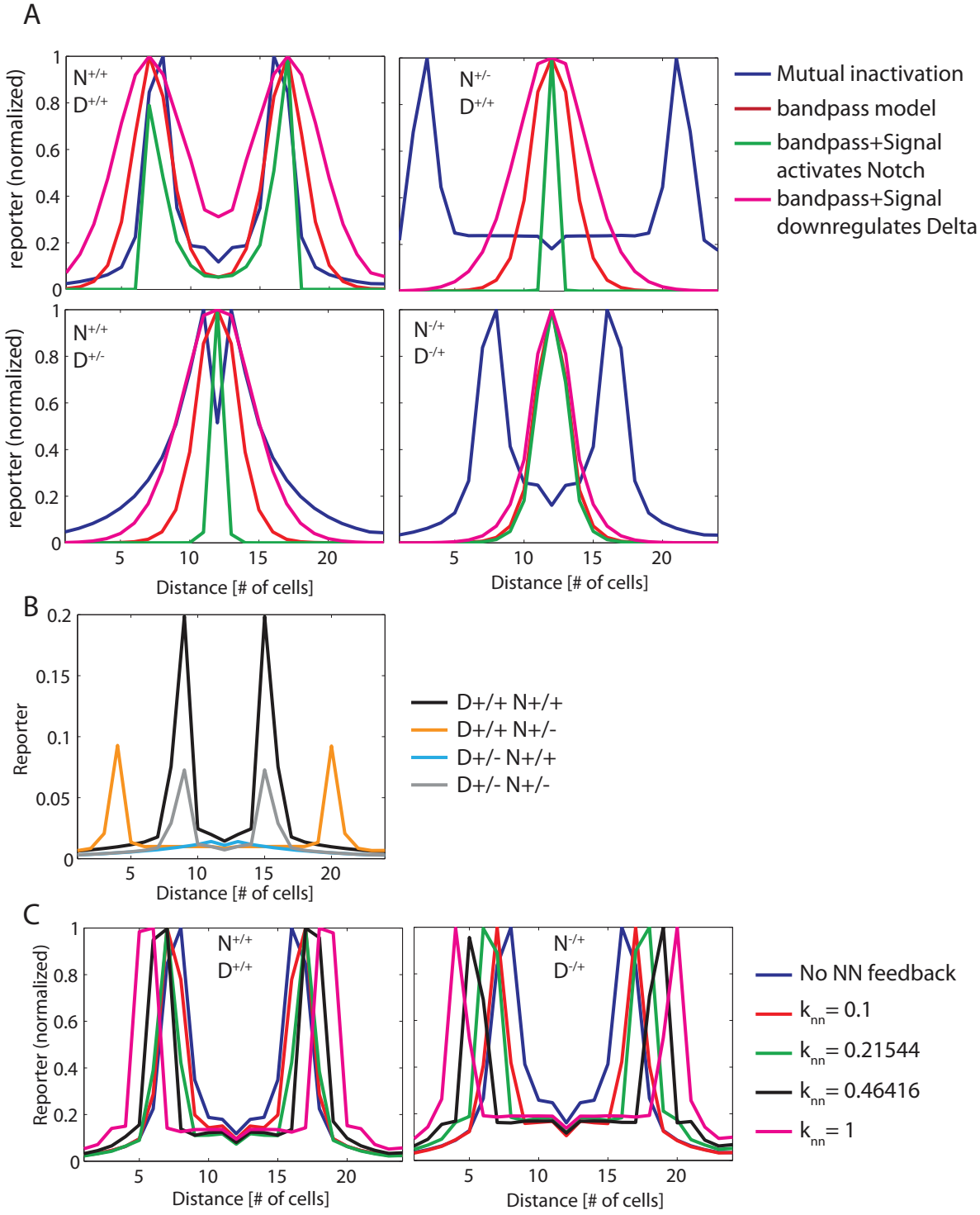

Figure S10: Comparison of the mutual inactivation model to alternative models of boundary formation. (A) Three alternative models are compared to the mutual inactivation model discussed in the main text (blue). The 'band-pass' model (red) assumes that the Notch target promoter responds only to a narrow range ("band") of Notch signaling levels. This band-pass function was represented by a product of activating and repressing Hill functions, each with Hill coefficient, *n*=8 (see section III of the supplementary modeling text). The high Hill coefficient is required to match the sharpness of the pattern generated with that obtained in the mutual inactivation model. For simplicity, no cis-inhibition was considered in this case. The second alternative model ("bandpass + signal activates Notch", green)

adds an additional transcriptional feedback of Notch signaling on the production rate of Notch, so that Notch signaling activates expression of Notch. Such feedback makes the outer edge of the pattern sharper. The third alternative model (magenta, "bandpass + signal downregulates Delta") adds feedback through Delta (Notch signaling downregulates production of Delta). This lateral inhibition type feedback tends to broaden the signal response. All models are defined in the supplementary theory section. See Table S3 for parameter values. Note that the two feedback models require fine tuning of the parameters to show a qualitative effect of the feedbacks (i.e. differentiate the feedback models from the simple bandpass). The four different panels correspond to Notch signaling profiles of the different models for N+/-, D+/-, and N+/- D+/- heterozygous mutants. All profiles were normalized to their maximal level to allow comparison of the boundary positions in different heterozygous mutant combinations. Top left corresponds to the wild-type case. Top right: Only the mutual inactivation model (blue) is consistent with the observed broad but sharp wing vein phenotypes of the N+/- mutant[3]. Bottom left: The D+/- phenotype of the mutual inactivation model (blue), but not the other models, shows broadening of the signaling profile (note the extended tails at a distance of ~5 cell diameters on the x-axis) and eliminates sharp side-bands (note that the central "dip" is an effect of the sharp kink in the morphogen profile at 0, and would not occur with a more realistic morphogen profile). These effects occur when the D+/- mutation makes the Delta production rate smaller than the Notch production rate. See also discussion in (B). Bottom right: In the mutual inactivation model, but not the other models, the double mutant N+/- D+/- regains the wild-type phenotype due to the ratiometric property discussed in Fig. 4D, Box 1, and in the text. This suppression is independent of the exact shape and length scale of the gradient. **(B)** Strong cis-inhibition selectively reduces signaling in the D+/- mutant. Here we plot the 4 un-normalized mutant profiles for the mutual inactivation model with a different parameter set (Table S3), with stronger cis-inhibition. The reporter level for the N+/+ D+/- mutant is substantially smaller than those of the wild type and all others mutants at all positions along the morphogen gradient. Such ubiquituous subthreshold activity of the reporter can be expected to resemble the null Delta phenotype of thicker and less sharply defined veins. Note that suppression in the double mutant persists for these new parameters, as shown by the invariance of the positions of the bands between wild-type and N+/- D+/-. More generally, suppression in the double mutant is maintained across a wide range of parameter values. **(C)** Positive feedback through Notch has a modest effect on suppression in the double mutant. Here we considered a variant of the mutual inactivation model in which Notch activity leads to increased expression of Notch. The strength of this feedback is quantified by the parameter k_{nn}, which denotes the amount of Notch signaling necessary to half-maximally induce the additional Notch production (supplementary theory section). Only intermediate values of k_{nn} change the spatial pattern (i.e. broaden it) without destroying its qualitative shape. Within this range, suppression is generally maintained except for a modest expansion (< ~1 cell) in the double mutant compared to wild-type.

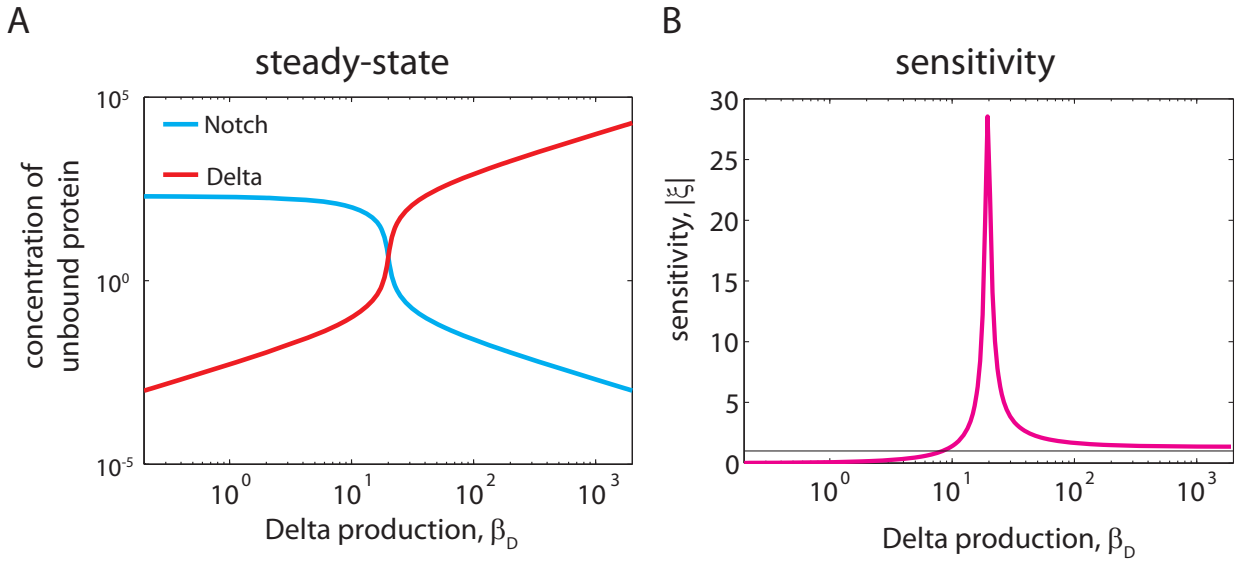

Figure S11: Steady-state sensitivity of the mutual inactivation switch. (A) The steady state levels of Notch (blue) and Delta (red) are shown with respect to the production rate of Delta, β_D, in a log-log plot, for the case presented in the Box Figure (values given in the Supplementary Table S3). This plot reveals a rapid change in Notch and Delta for a small change in the β_D near the switch location. (B) Steady-state sensitivity of the system, as defined in Box 1, for the conditions of plot A. Note that the sensitivity of the system remains larger than 1 for a very broad range of Delta production rates (to the right of the threshold).

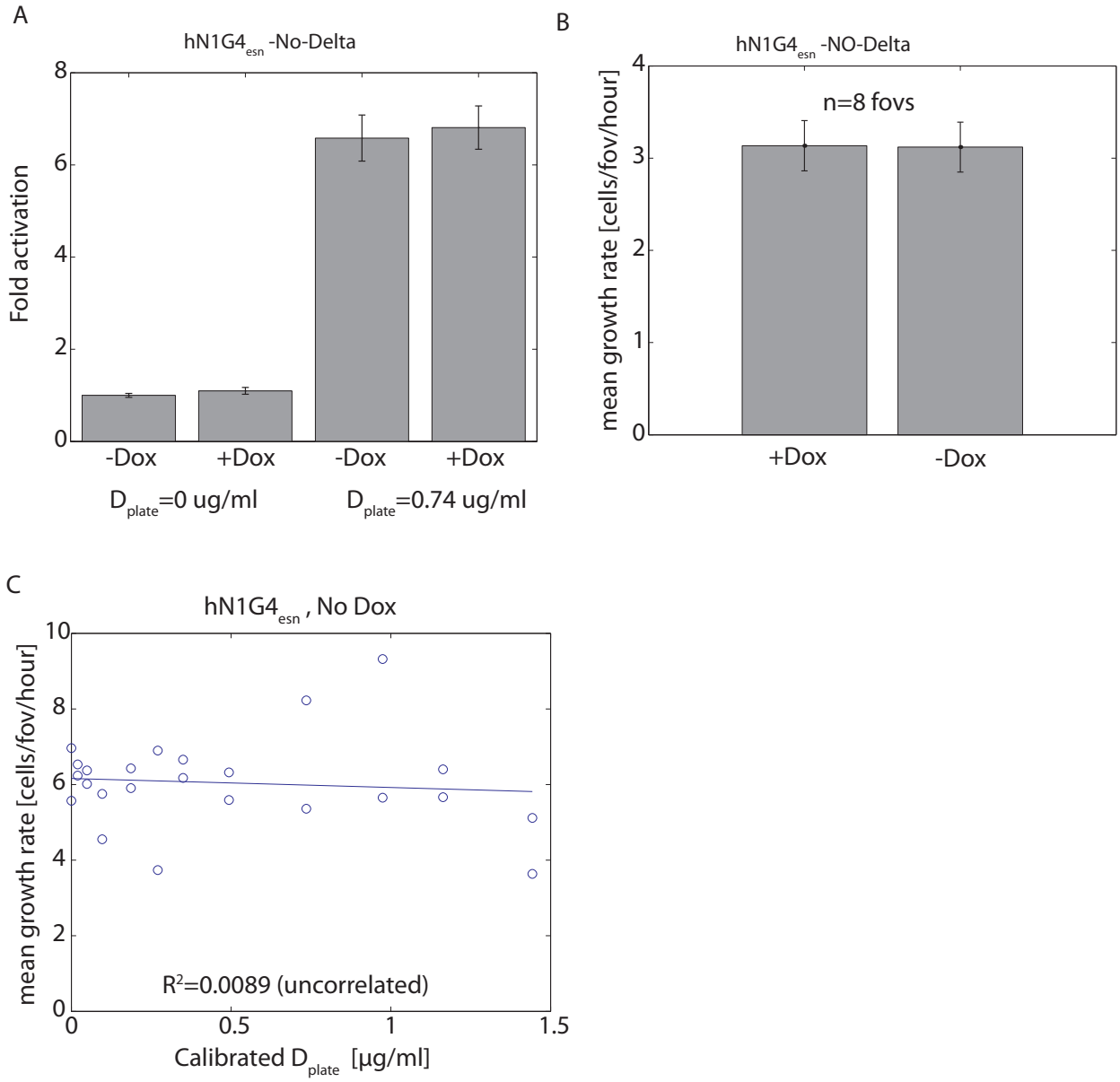

Figure S12: Negative controls show that Notch signaling is not affected by doxycycline, and growth rate is not affected by doxycycline and D_{plate}. (A) Cells expressing Notch (hN1G4esn -No-Delta) were induced by D_{plate} to similar levels of Notch activity in the presence or absence of 100ng/ml doxycycline (protocol was similar to the ones used in Fig.2), showing that Notch activity is not influenced directly by doxycycine. (B) The growth rate of the Notch reporter cells was not affected by presence of doxycycline. (C) Mean growth rate of the cells shown in Fig. 2C,D,E is not affected by D_{plate}. Growth rate was defined as the rate of increase in the number of cells per field of view (fov) over time.

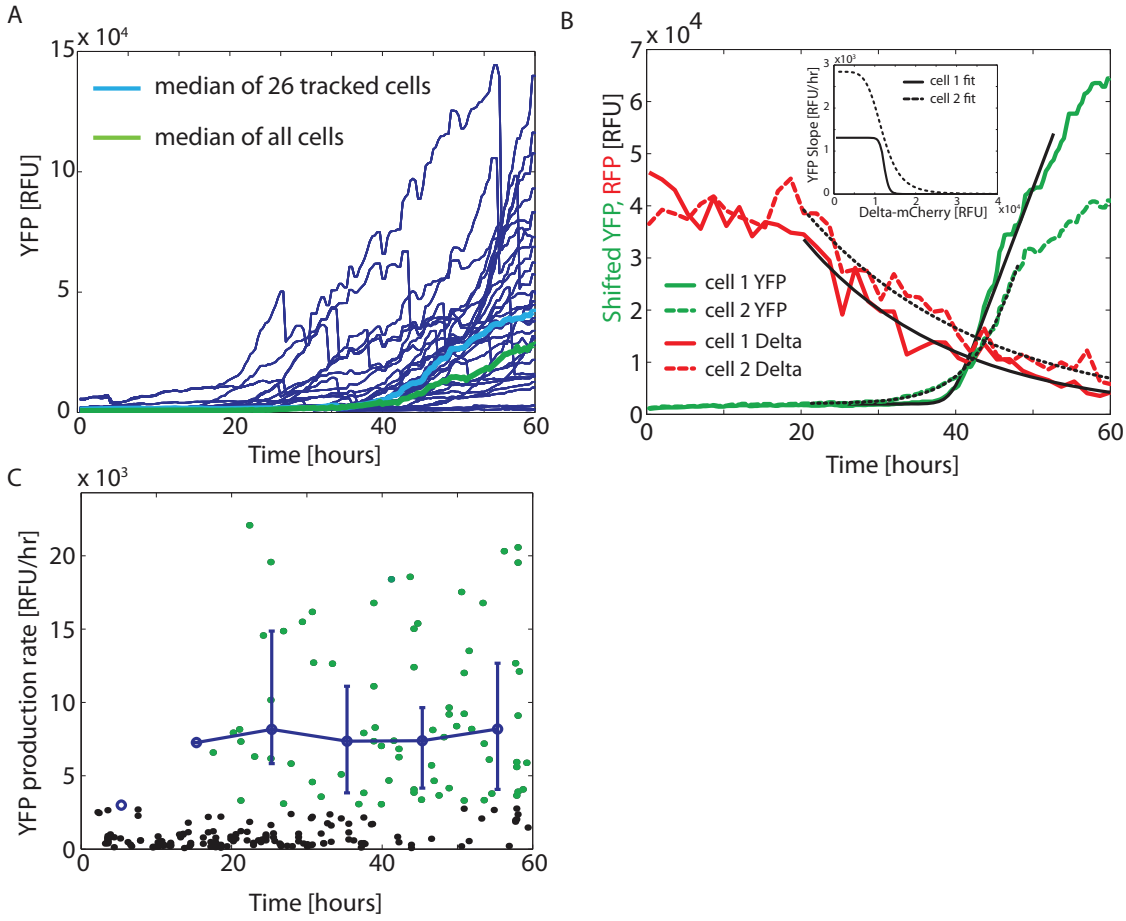

Figure S13: Relation of population average data (median over all segmented cells) and single cell data. (A) Plots of total cellular fluorescence versus time for each of 26 non-overlapping cell lineages from the movie shown in Figs. 3B, (blue lines). Sudden drops in total fluorescence are due to cell division events, as in Fig. 3D. We compare the median of these 26 responses (cyan) to the median over all cells (green). Note that this latter curve is identical to that shown in Fig. 3. For discussion see supplementary methods. (B) Analysis of sharp responses to cis-Delta in individual cells. The concentration of Delta-mCherry (red) and the shifted level of YFP (green, cf. Fig. 3e) are plotted as a function of time for two different cell lineages. Delta-mCherry concentrations were estimated from total Delta-mCherry fluorescence levels by assuming linear growth in cell volume during each cell cycle. The Delta-mCherry data were fit to exponential decays (superimposed black lines). The YFP response curves were fit to generate the turn-on function (superimposed black lines). The fit has four free parameters: a constant offset, a final slope, a turn-on time (t_{on}), and τ_{rise} (see supplementary methods). Inset: plots of resulting Hill function fits for the production rate of YFP as a function of the concentration of Delta-mCherry. These fits produced best fit Hill coefficients of n=22±10 and n=5.5±0.8 for cells 1 and 2, respectively. (C) Analysis of slope distributions of cis-Delta response shows a switch-like, rather than graded behavior. All 26 single cell traces were divided into short, 6 hour segments. The response on each segment was smoothed and its maximal slope was measured. Black and green points represent the values of individual slopes falling below or above a threshold, respectively. Note that the fraction of activated (green) points, but not their median value, increases over time, consistent with a switch-like model (Fig. 5e). The threshold value was determined from the early time points where cells are off. A few segments far from the switching point were filtered out, corresponding to saturating fluorescence levels or varying YFP expression at very late times (YFP curves in (b)). Similar filtering did not affect the distribution of trans-activation rates (Fig S5g). Blue circles represent the medians of the individual above-threshold (green) slopes in 30 hour bins. Error bars represent the 25th to 75th percentiles of each distribution. Comparison with trans-Delta distributions (Figs. S5e,f,g) shows that the response to cis-Delta agrees with a threshold like model.

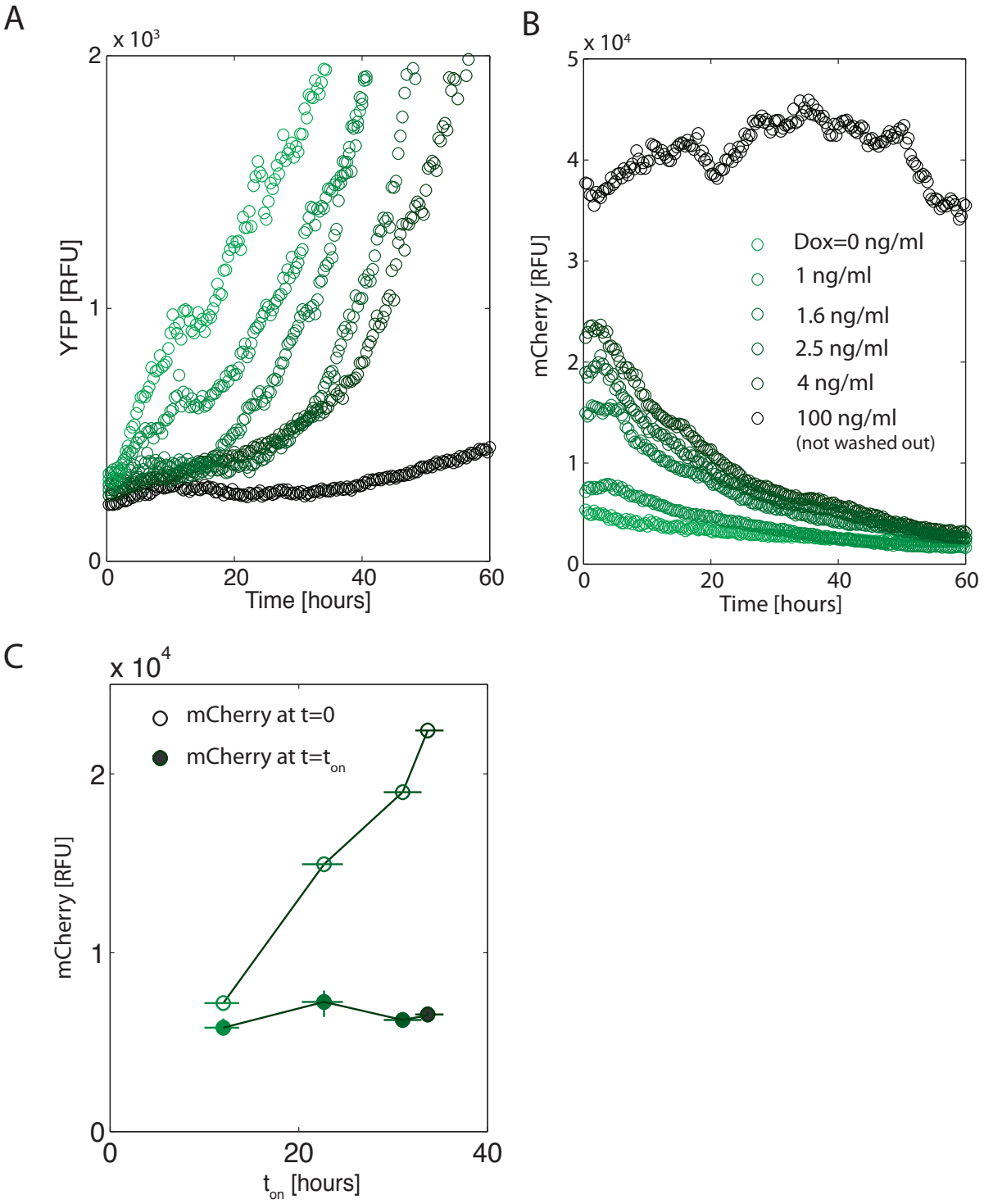

Figure S14: Initial Delta-mCherry levels correlate with turn-on time. (A) Notch signaling response was measured for varying Delta-mCherry induction levels. The experimental setup was similar to the scheme shown in Fig. 3A. Cells were grown on fixed D_{plate}=0.74 ug/ml and subjected to 12 hour pulses of varying doxycycline concentrations, as indicated in (B). Increased induction levels correspond to higher Delta-mCherry induction (B) and corresponding delays in the turn-on time (A). When doxycycline is not removed from the media (darkest green), cells show a negligible response to D_{plate}. (C) Here, t_{on} was calculated for the data in (A) and (B). For each Delta-mCherry induction level (same legend as in (B)), the Delta-mCherry fluorescence at the start of the movie (t=0) and at t_{on} are plotted. These data show that the time of Notch activation, t_{on}, varies with the initial level of Delta-mCherry expression, but occurs at an approximately constant Delta-mCherry concentration, as expected from the experimental scheme in Fig. 3A. Note that fluorescence levels differ in this figure from those in Fig. S13 due to variations in optical parameters (e.g. lamp intensity) between the two experiments.

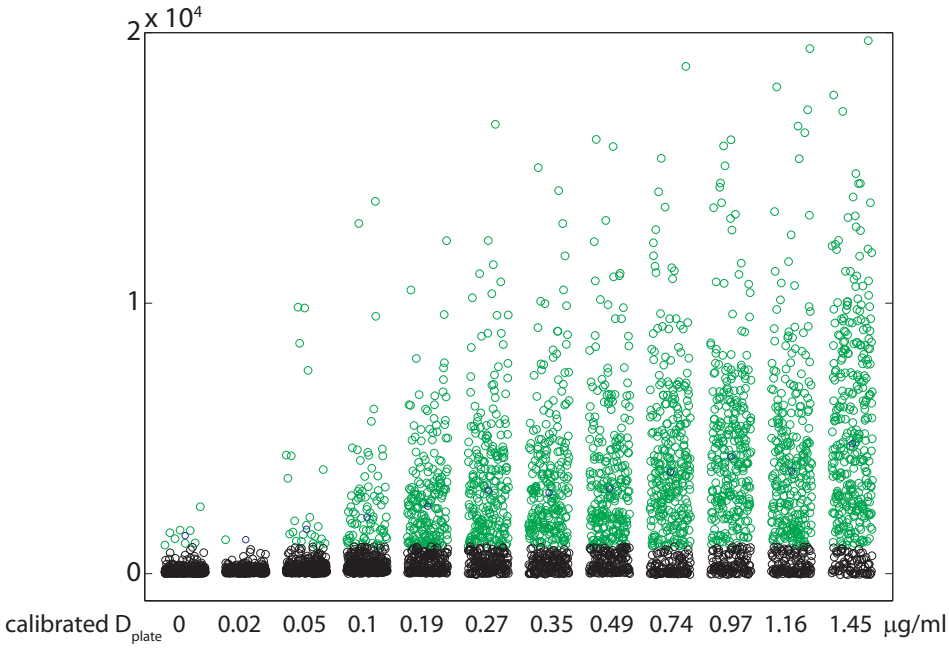

Figure S15: Distribution of activated cells at different D_{plate} shows graded response. Distributions of hN1G4^{esn} cells after onset of induction (t=50 hours) in Figure 3G. Activated cells (green circles) respond in a graded fashion to D_{plate} levels. Note that even at maximal activation there is a fraction of non-responding cells (black circles). Such variable behavior typically occurs due to silencing of viral promoters such as the CMV promoter used here. The blue circles represent the median of activated cells. Note that in figure 2C we plot the median of all cells (green and black circles). The median of all cells exhibits a similar slope to the median of activated cells at longer times, but it shows an initial lag in the response. This lag occurs since the median of all cells remains unchanged until more than 50% of the cells respond to D_{plate}. See also discussion in Fig. S5.

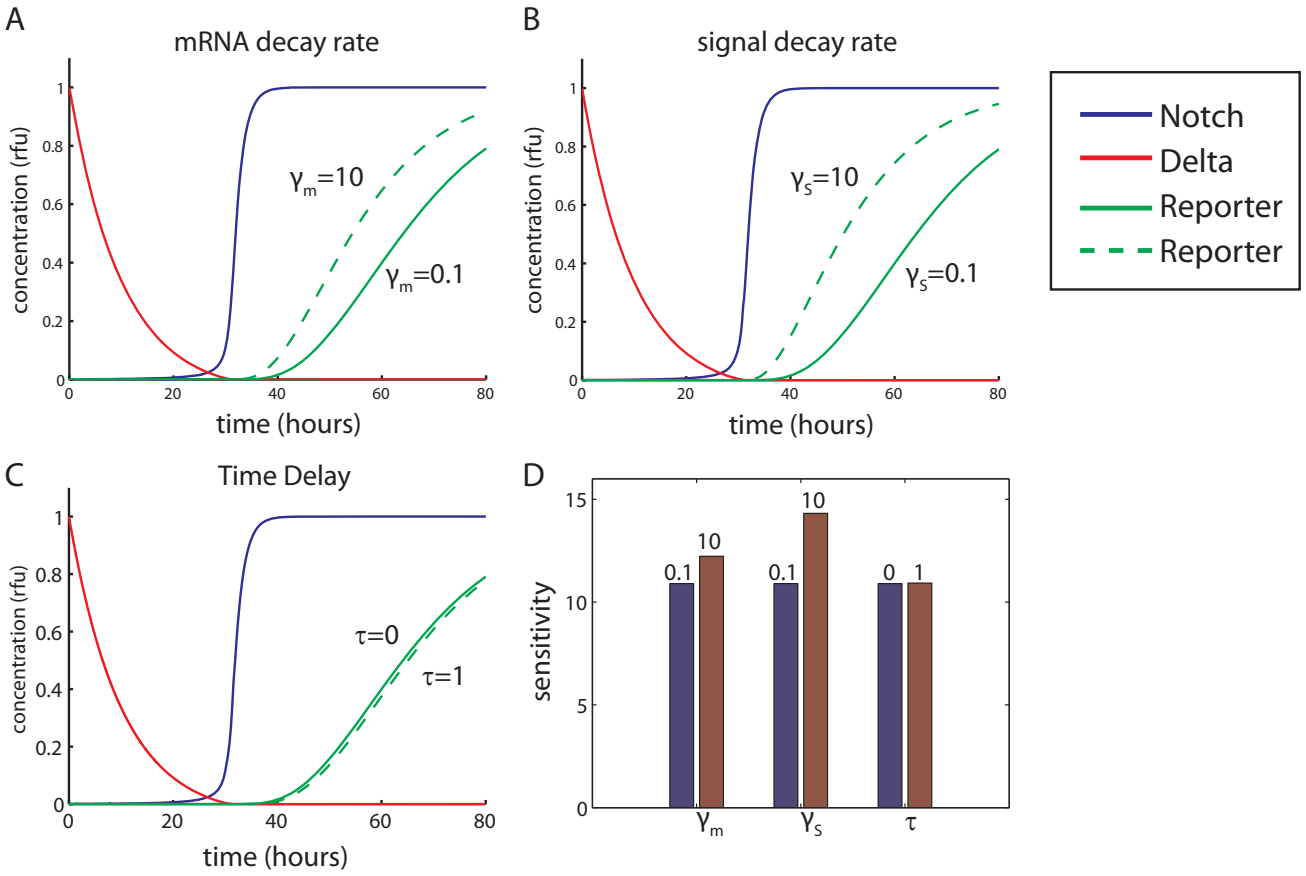

Figure S16: Effect of finite lifetimes and expression delays in the model. Time traces of Notch (blue), Delta (red), and the reporter (green) obtained from numerical simulations of the *cis*-inhibition model. Solid and dashed green lines are reporter traces for different parameter values, indicated on plot. (A) A 100x increase in the lifetime of the reporter mRNA leads to a delay of a few hours in the turn-on of reporter expression. (B) A similar effect is found for a 100x increase in the lifetime of the Signal. (C) A 1-hour delay in the expression of the reporter from the activating signal leads to a corresponding delay in reporter turn-on. (D) Despite these time shifts, the dynamic sensitivity of the system, defined as the logarithmic derivative of the Signal with respect to the total amount of Delta at any given time instant, is mostly unchanged. The sensitivity coefficient, shown in the bar plot for the different cases presented in plots A-C, increases at most 30% for the smallest lifetimes, and is effectively constant in the presence of delay in the reporter expression.

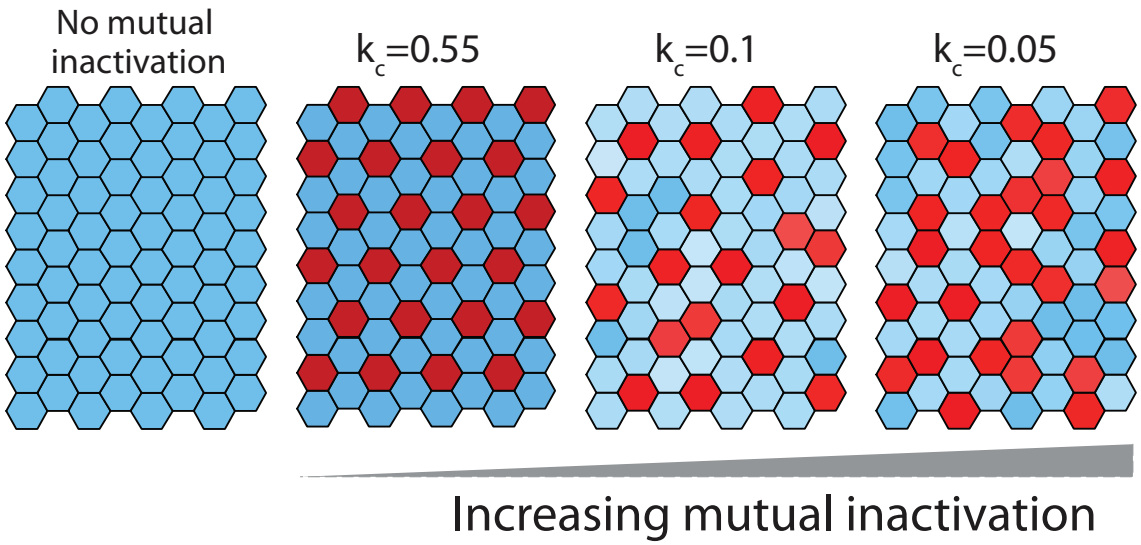

Figure S17: Lateral inhibition model with mutual inactivation (See theoretical supplementary section) facilitates broader range of patterns. Increasing the strength of mutual inactivation (reduced k_c) enables patterning (second panel), as well as the formation of alternative patterns in which cells with high Delta levels can stably co-exist next to each other (third and fourth panels). Such alternative patterns cannot be achieved using standard lateral inhibition model (even in the presence of cooperative feedback).

Supplementary Methods

Description of genetic constructs

All genetic constructs used in this paper were constructed using standard cloning and PCR techniques. All constructs were fully sequenced and the maps, sequences and construction details are available upon request. We provide below a description of the sources for vectors and DNA fragments used, as well as the main construction steps.

Reporter plasmids pEV-UAS-H2B-Citrine and pEV-12xCSL-H2B-Citrine were constructed as follows: The backbone vector pEV was constructed in the lab by amplifying pSecTagA without the secretion tag Murine Ig kappa-chain V-J2-C (Invitrogen, V900-20) and religating it with the *Sac*II restriction site. The UAS-H2B-citrine and 12xCSL-H2B-Citrine were amplified or subcloned from earlier constructs and they contain the following DNA fragments: H2B-citrine originally obtained from pCS H2B citrine (a gift from Sean Megason and Scott Fraser[4]). UAS was obtained from ULyn-GFP (a gift from Scott Fraser[5]). 12xCSL was amplified from 12xCSL DsRedExpress (a gift from Urban Lendahl[6]).

pcDNA3-hN1-mod1 was constructed by first adding an *Nhe*I site to pcDNA3 hN1 (a gift from Jon Aster[7]). To add this *Nhe*I site we amplified the DNA fragment between the *Not*I to the *Xho*I site and included the *Nhe*I site in the reverse primer. The resulting amplicon was ligated into pcDNA3-hNI cut with the same restriction sites. This modified plasmid was then used to create pcDNA3-hN1-mCherry by inserting mCherry originally amplified from pFA6-link-mcherry-SpHis5 (a gift from Roger Tsien and Kurt Thorn[8,9]) into the *Nhe*I and *Xho*I sites.

pcDNA3-hNECD-Gal4^{esn} was constructed by cutting pcDNA3-hN1-mod1 with *Not*I and *Xho*I to remove hNICD. Gal4^{esn} was constructed by PCR amplification from S*accharomyces cerevisiae* as described in Ptashne et al [10]. Gal4^{esn} amplified with *Not*I and *Sal*I restriction sites was inserted into the cut vector in the sites above. We note here that Gal4^{esn} was chosen over the more popular Gal4-VP16, since it does not use the viral activator VP16 which is extremely strong and generates high background signal.

pcDNA5/TO-hNICD-Gal4^{esn} was constructed using the pcDNA5/TO vector (Invitrogen , V1033-20) cut with *Bam*HI and *Not*I and by amplifying hNICD-Gal4^{esn} with the same restriction sites from pcDNA3-hN1-Gal4esn (a construct not used here but was constructed by introducing Gal4esn into pcDNA3-hN1-mod1).

pcDNA5/TO-Delta-mCherry was constructed by first modifying pcDNA5/TO (Invitrogen, V1033-20) to add a *Nhe*I restriction site by cutting with *Hin*dIII and *Bam*HI and then ligating in 2 annealed oligos, which contained the *Nhe*I site. The vector was then digested with *Nhe*I and *Bam*HI. Delta-mCherry was cut from a previously constructed vector with the same restriction sites as pcDNA5/TO. Delta originally came from pBOS-rDelta1[11] (a gift from Gerry Weinmaster) and was fused to mCherry using fusion PCR. The overlapping sequence between the two fused proteins is: GTGTTATAGCGACTGAGGTTgtgagcaagggcgaggagga.

pcDNA5/TO-Gal4^{esn} was constructed by removal of the mCherry from pcDNA5/TO-Gal4^{esn}-mCherry through BamHI and NotI digestion. A small DNA fragment (made from annealed oligos) containing a stop codon as well as the BamHI and NotI overhangs was ligated into the cut pcDNA5/TO-Gal4^{esn}-mCherry vector. The pcDNA5/TO-Gal4^{esn}-mCherry vector was originally created by first performing a fusion PCR of Gal4^{esn} and mCherry (sources for Gal4^{esn} and mCherry previously described). The PCR product was ligated into the pcDNA5/TO vector from Invitrogen.

pCS-H2B-cerulean was a gift from Sean Megason and Scott Fraser[4].

pcDNA6-UAS-H2B-Citrine was constructed by subcloning UAS-H2B-citrine from pEV-UAS-H2B-Citrine into pcDNA6/ V5-HisA (Invitrogen, V220-01) using *Mfe*I and *Bst*BI restriction sites.

pEV-12xCSL-H2B-mcherry was constructed by amplifying the 12xCSL promoter from 12xCSL DsRedExpress then fusing it to H2B-mCherry.The resulting amplicon was digested with *Mfe*I and *Bgl*II and inserted into pEV between *Mfe*I and *Bam*HI. H2B-mCherry was constructed by fusion PCR of H2B and mCherry fragments.

Generation of stable cell lines and cell-culture protocols

As a base cell line we used T-REx-CHO-K1 cells (Chinese Hamster Ovary cells supporting the T-REx inducible system, Invitrogen) which were grown in Alpha MEM Earle's Salts (Irvine Scientific) supplemented with 10% Tet System Approved FBS (Clontech), 100 U/ml penicillin -100 ug/ml streptomycin – 0.292 mg/ml L-glutamine (Gibco), and 10 ug/ml Blasticidin (InvivoGen) at 37^{o}C in the presence of 5% CO_2 under a humidified atmosphere. For construction of stable cell lines, cells were plated 24 h prior to transfection in 24 well tissue culture treated plates such that 80-95% confluency would be reached by the time of transfection. Cells were transfected using Lipofectamine 2000 (Invitrogen) as per the manufacturer's instructions. The amount of total DNA used was 800 ng/well: 100 ng of DNA containing the desired cassette + 700 ng empty plasmid (pOri).

Stable cell lines containing either the 12xCSL-H2B-Citrine or UAS-H2B-Citrine reporters were created by transfection of pEV-12xCSL-H2B-Citrine or pEV-UAS-H2B-Citrine into T-REx-CHO-K1 cells. A plasmid containing H2B-Cerulean under constitutive CMV promoter (pCS-H2B-Cerulean) was co-transfected together with the pEV-UAS-H2B-Citrine. Positive cells were selected by replating transfected cells into 6 well tissue culture treated plates with media containing 400 ug/ml Zeocin (Invitrogen) and 10 ug/ml Blasticidin 24 h post-transfection. Cells transfected with DNA lacking an antibiotic resistance gene were used as a control to monitor positive cell selection. After the control cells died, and after several passages of the selecting cells, positive cell populations were either sorted by FACS (FACSAria, Beckman Dickinson) or diluted in 96 well tissue culture treated plates in order to obtain single clones to test for reporter activity. For FACS, cells were transiently transfected with pEF-GV-ICD (a plasmid containing a fusion of Gal4-VP16 and Notch ICD) 24 h prior to cell analysis and sorting. Individual cells expressing high levels of citrine were sorted into single wells in a 96 well tissue culture treated plates. Alternatively, positive cell populations were plated into 96 well tissue culture treated plates at 0.2 cells/well in order to increase the likelihood of obtaining a single cell/well. Individual cells were grown in selection media until enough cells were available to test reporter activity. Each clonal cell population was tested by

transient transfection with pEF-GV-ICD, and clones with the best dynamic range of reporter induction were identified by microscopy and used for the next round of stable cell line creation.

For the addition of Notch constructs into the two stable reporter cell lines constructed above, plasmids containing either hN1 fused to mCherry (pcDNA3-hN1-mCherry) or hN1G4^{esn} (pcDNA3-hNECD-Gal4esn) were transfected into the 12xCSL-H2B-Citrine or UAS-H2B-Citrine reporter cell lines, respectively. Positive cell populations were selected as previously described with selection media that contained 400 μg/ml Zeocin, 10 μg/ml Blasticidin, and 600 μg/ml Geneticin (Invitrogen). Clonal cell populations were obtained by FACS or dilution as detailed above. Positive cell populations used for FACS were plated in wells treated with 2.5 μg/ml IgG-Delta^{ext} 48 hours before sorting. Individual cells expressing high levels of citrine were sorted. Clones were tested by plating cells in wells treated with or without 2.5 μg/ml IgG-Delta^{ext} and monitoring activation of the 12xCSL-H2B-Citrine or UAS-H2B-Citrine reporter by microscopy 48-72 hours post-Delta exposure. Single hN1 and hN1G4^{esn} clones with minimal H2B-Citrine background expression and high reporter activation when exposed to Delta were selected for further use.

To create the final cell lines hN1 and hN1G4^{esn} shown schematically in Figs. 1C, S1, a plasmid expressing Dl-mCherry under an inducible promoter (pcDNA-TO-Dl-mCherry) was transfected into each of these cell lines. A plasmid containing H2B-Cerulean under constitutive CMV promoter (pCS-H2B-Cerulean) was co-transfected with the Delta-mCherry into the hN1 cell line. Cells were grown in selection media containing 400 μg/ml Zeocin, 10 μg/ml Blasticidin, 600 μg/ml Geneticin, and 500 μg/ml Hygromycin (InvivoGen) for each of the hN1 cell lines. After selection, cells were either treated with 1 μg/ml doxycyclin and subjected to FACS or diluted into 96 well tissue culture treated plates as previously described. For FACS, single cells expressing high levels of mCherry were sorted. Clonal cell populations were grown and tested for low mCherry background expression in the absence of doxycycline and good inducibility of mCherry expression when exposed to 1 μg/ml doxycycline. Optimal clones for each of the above cell lines were identified by microscopy and used in further experiments.

A separate cell line containing only inducible Delta-mCherry (used in co-culture experiments), was created by transfecting T-REx-CHO-K1 cells with pcDNA-TO-Dl-mCherry. Clones were generated in a similar process as above albeit with a selection media containing only Blasticidin and Hygromycin. This cell line was used to generate the TO-DMC+hN1G4^{esn} used in Fig. S9 by stably transfecting into it the pcDNA3-hNECD-Gal4esn construct (600 μg/ml Geneticin). *We note that the fusion to mCherry could in principle affect various activities of Delta. Therefore, we verified that Delta-mCherry can trans-activate Notch reporter cells efficiently (as shown in Fig. S3). This does not rule out the possibility that other activities or properties of Delta may be affected by the fusion.*

For creation of the TO-Gal4^{esn} cell line, the UAS-H2B-Citrine + CMV-H2B-Cerulean cell line was transfected with the pcDNA5/TO-Gal4^{esn} plasmid. Cells were grown in selection media containing 400 μg/ml Zeocin, 10 μg/ml Blasticidin, and 500 μg/ml Hygromycin. After selection, cells were diluted into 96 well tissue culture treated plates to obtain single clones. Clones were tested for Gal4^{esn} inducibility by plating cells either with or without 1 ug/ml doxycycline. The clone with the lowest Citrine

background expression in the absence of doxycycline and good inducible Citrine expression in the presence of doxycycline was chosen for further use in experiments.

For production of a double reporter cell line used in Figure S1, CHO-K1 cells (without T-REx, ATCC, CCL-61) were first transfected with pcDNA-UAS-H2B-Cit. A positive cell population was selected with media containing 10 μg/ml Blasticidin. After the initial selection, positive clones were obtained by FACS as previously described for the individual reporter stable cell lines. Each clone was then tested by transfection with pEF-GV-ICD, and a clone with the best reporter dynamic range was identified by microscopy and used to transfect in pEV-12xCSL-H2B-mCherry. Transfected cells were selected in media containing 10 μg/ml Blasticidin and 400 μg/ml Zeocin. A positive double reporter clone was identified by the method described above. In the clone chosen for further experiments, both reporters showed minimal background activation and high levels of Citrine and mCherry when transfected with pEF-GV-ICD.

Measurements of relative Notch expression levels in hN1G4^{esn} and hN1

To estimate the levels of ectopically expressed Notch receptors in the hN1G4esn and hN1 we performed qRT-PCR on the two cell lines in which levels of Notch mRNA were compared to levels of endogenous β-actin mRNA. We found Notch levels 2.3 ± 0.15 and 4.5 ± 0.4-fold smaller than those of β-actin in the hN1G4^{esn} and hN1 cell lines , respectively. These results are within the physiological range of endogenous Notch receptors as observed in early T-cell progenitors where Notch is active[12]. See below for details of qRT-PCR analysis.

Description of experimental protocols and microscopy

Delta plating, preparation of cells for imaging, and calibration assay for IgG-Delta^{ext}.

Protocol for setting up a time lapse movie: Cells were plated on a glass bottom 24 well plate (Mattek). To bind IgG-Delta^{ext} to the plate, IgG-Delta^{ext} was serially diluted to different concentrations in cold 1xPBS (Invitrogen) containing 5μg/ml hamster fibronectin (Innovative Research). 500μl of diluted IgG-Delta^{ext} was incubated at 4°C for 1 hour on a rocker. Cells were trypsinized and diluted to 2x10^4 cells/ml (1x10^5 cells/ml for coculture experiments) in growth medium containing 100ng/ml doxycycline (Sigma Aldrich). The cells were plated immediately after the incubation onto the 24 well plate containing IgG-Delta^{ext}. Prior to imaging, wells were washed twice with fresh media and media was replaced with low fluorescence imaging media αMEM without Phenol red, riboflavin, folic acid, and vitamin B12 (Invitrogen, custom made) and with 5% FBS and 1% L-glutamine+Penicilin-Streptomycin 100x mix (Invitrogen). Calibration of the IgG-Delta^{ext} bound to the plates is discussed in the captions of Fig. S4.

Microscopy details:

Cells were imaged in an Olympus IX81-ZDC microscope equipped with an ASI 2000XY stage and a cooled back-thinned iKon-M CCD camera (Andor). All movies were taken with a 20x, 0.7NA objective. The microscope is also equipped with an incubator that maintains the temperature at 37C and with an environmental chamber with a humidified 5% CO2 flow (custom made). The microscopy setup is

automatically controlled using commercial Metamorph (Molecular Devices) software. 48 stage positions (2 in each well) are set up manually and their coordinates are stored in the computer. In each position, the program first focuses using the Zero Drift Control module (Olympus Inc.), then takes a DIC image, and three fluorescent images (mCherry, citrine, CFP). Images are taken every 20 minutes for all positions. Typical total movie time is approximately 48 hours.

Western Blot:

TO-Gal4esn cells were plated in wells of a 6-well tissue culture treated plate at 5x105 cells/well. The cells were induced with 100 ng/ml of doxycycline. After 24 hr of induction, one well of cells was harvested (0 hr post-doxycycline removal) while the doxycycline was washed out of 4 additional wells. Those cells were harvested at 1 hr, 2hr, 4 hr and 6hr post-doxycycline removal (an uninduced sample was used as a control). The harvested cells were counted, and 4x106cells were pelleted and lysed with 200ul 1.5x complete SDS loading buffer (76.7 mM Tris-HCL, pH 6.8, 1.5% (w/v) SDS, 15% (v/v) Glycerol, 0.01% (w/v) Bromophenol blue, 30 mM Dithiothreitol (DTT), 213.8 mM 2-Mercaptoethanol, 1x protease inhibitors (Roche Applied Science), 6 mM ethylenediaminetetraacetic acid (EDTA)). Cellular extracts were boiled for 5 min at 95ºC, vortexed, chilled on ice and centrifuged in a Beckman TLA-100.3 ultracentrifuge rotor at 55,000 rpm for 1 h at 4ºC. For each sample, 10ul of supernatant was resolved in triplicate on a NuPAGE Novex 4-12% Bis-Tris Midi Gel (Invitrogen) and transferred to a 0.2 µm nitrocellulose membrane using the iBlot from Invitrogen (a standard curve made from serial dilutions of the 0 hr post-doxycycline sample was also included on the gel). The membrane was blocked with 5% (w/v) dry milk and 2% (w/v) BSA in 1xTBST (20 mM Tris base, 137 mM sodium chloride, 0.1% (v/v) Tween 20, pH 7.6), incubated with primary antibody in blocking buffer, followed by incubation with horseradish peroxidase-labeled secondary antibody in blocking buffer. SuperSignal West Femto chemiluminescent substrate kit was used for detection (Pierce). The following primary antibody was used: rabbit anti-Gal4 DBD (sc-577, Santa Cruz Biotechnology, 1:200). The secondary antibody used was horseradish peroxidase linked anti-rabbit IgG (Amersham, 1:2000). Protein bands were visualized on a VersaDoc gel imaging system (Bio-Rad Laboratories).

qRT-PCR:

Notch mRNA levels in the hN1 and hN1G4esn cells were compared to endogenous Notch mRNA observed in early T-cell progenitors. RNA was isolated from hN1 and hN1G4esn cells using the RNeasy kit (Qiagen). cDNA was subsequently synthesized from 1µg of RNA using the iScript cDNA Synthesis kit (Bio-Rad). From a 20ul reaction, 2ul of cDNA was used to assess Notch and β-Actin mRNA levels using real-time qRT-PCR. Primer and probe sets used were as follows: hNotch1, forward 5'-ATGAGTTCCAGTGCGAGT-3', reverse 5'-TGTAAGTGTTGGGTCCGT-3', probe 5'-FAM-AGATGCCCAGTGAAGCCCGT-Blk_FQ-3'; β-actin, forward 5'-ACTGGGACGATATGGAGAAG-3', reverse 5'-GGTCATCTTTTCACGGTTGG-3', probe 5'-HEX-ACCACACCTTCTACAACGAGCTGC- Blk_FQ-3'.

Flow cytometry:

TO-DMC or TO-DMC+ hN1G4^{esn} "sending" cells were co-cultured with hN1G4^{esn}-No-Delta "receiving" cells in a transactivation assay. Co-cultures were plated at 10^5 cells/well in a 24 well plate at

a ratio of 20% Delta cells to 80% Notch reporter cells. For each set of co-cultures, a 12 hr pulse of 1.6 ng/ml and 100 ng/ml doxycycline was performed (a well with no doxycycline served as a control). After doxycycline removal, the cells were washed 3x with 1xPBS (GIBCO) followed by addition of growth medium. Cells were incubated at 37^{o}C, 5% CO_2 for an additional 24 hr before harvesting for flow cytometry analysis. Cells were trypsinized and diluted in 500µl analysis buffer (1x Hank's Balanced Salt Solution (GIBCO), 2.5 mg/ml BSA (w/v)). After filtering through a 40µm mesh, the co-cultured cells were analyzed for YFP fluorescence using a FACScalibur flow cytometer (Becton Dickinson).

Image and data analysis

Segmentation of images

CFP images were used for automated segmentation of each frame of the movie. Segmentation was performed in a similar manner to previously described methods [2]. Briefly, each image was first subjected to an edge detection algorithm using Matlab. Closed edges were selected and several morphological and intensity criteria including total pixel area and mean fluorescence intensity level were used to identify the nuclei of the cells. The segmented image was used as a mask to calculate YFP and CFP fluorescence as well as centroid position for each nucleus. In some cases manual correction was applied to the segmented images. mCherry levels for the single cell tracks in Fig. 3E were obtained by manual segmentation of the entire cell, in order to include total mCherry fluorescence.

Generating population averaged response curves

To generate the YFP response curve for each movie (such as the ones in Figs. 2C and 3C), the total YFP fluorescence of each cell was calculated and background fluorescence was subtracted. Each data point on Figs. 2C and 3C represent the median of this total fluorescence per cell over all cells of one frame in the movie. The median, rather than the mean, was used for two reasons: (1) The median is less sensitive to occasional bright outliers such as dead cells and multinucleated cells which may offset the mean. (2) Median fluorescence taken in each frame roughly follows the response of the median cell lineage (see below), and thus better captures the sharp turn on feature shown in Fig. 3C-H. As shown in Fig. S13, the median curve essentially follows one of the single cell tracks for a while before switching to the next median curve. Hence, for such 'turn-on response' as in Fig. 3C, the median curve stays low until half the cells switch on. It then assumes a slope similar to that of the cells that have already responded. Thus, the rise time of the median curve provides a much better estimation of the median of the single cell lineage rise times than does the rise time of the mean curve (not shown).

The mean Delta-mCherry decay curve in Fig. 3C was calculated by taking the total mCherry level above background for each frame and dividing by the number of cells in that frame.

Single cell tracking was performed using a modified version of the Soft Assign algorithm [2,13] and was verified and corrected manually for each cell lineage tracked.

Data analysis

Hill coefficients on Figs 2D, S1 were obtained by fitting the data to a Hill function of the form $y = A\frac{x^n}{K+x^n}$ where x is the D_{plate} value, y is the YFP production rate value, and A, K, and n are free fitting parameters. The fit was performed using a weighted non-linear least squares algorithm (Matlab). The weights vector was taken to be $\frac{1}{k+y_i}$, where y_i is the production rate value for the i^{th} data point and k is a minimal error parameter (typically 10% of $max(y_i)$). This weighting takes into account both logarithmic errors (assuming a log-normal distribution of y_i's) and smaller fixed errors (i.e errors not proportional to y_i levels).We verified that the value obtained for the Hill coefficients, n, was not sensitive to the exact fitting procedure and parameters.

The single cell rise times for the distribution obtained in Fig. 3F were calculated by fitting the shifted YFP curves (such as the ones in Fig. 3E) to the following functional form:

$$(1) \qquad y(t) = S(t + \frac{1}{\gamma}\ln\left(\frac{1+exp(-\gamma(t-t_c))}{1+exp(\gamma t_c)}\right) + c$$

Here, y represent the shifted YFP fluorescence level, t represent time, t_c is the time at which the response turns on (i.e the 'knee'), γ, quantifies the sharpness of turn-on, *S* is the maximal slope at $> t_c$, and $c = y(0)$ is a constant.

This functional form is derived in the following way: We first assume an effective Hill function response of the production rate of YFP (dy/dt) to the level of Delta-mCherry (DMC):

$$(2) \qquad \frac{dy}{dt} = S\frac{k_d^m}{k_d^m+(DMC)^m}$$

Here, m and k_d represent the effective Hill coefficient and the Delta-mCherry value that gives half-maximal expression, respectively. We assume an exponential decay of Delta-mCherry (i.e. D_{cis}): $DMC = D_0\, exp(-\gamma_0 t)$ where $D_0$and γ_0 are initial Delta-mCherry level and degradation rate, respectively. Hence the YFP production rate as a function of time is given by:

$$(3) \qquad \frac{dy}{dt} = S\frac{1}{1+exp(-\gamma(t-t_c))}$$

Here, $\gamma = m\gamma_0$, and $exp(\gamma t_c) = \left(\frac{D_0}{k_d}\right)^m$, The functional form in eq. (1) is obtained by integrating eq. (2) over time. Fitting of the data to eq. (1) was performed similarly to the Hill function fits described above. The rise time is then given by $\tau_{rise} = 2/\gamma$. We note that while eq. (1) is only an approximation to the actual response curve it fits the data well and enables estimation of rise times in simulated data.

Supplementary references

1 Franco, C. B. *et al.* Notch/Delta signaling constrains reengineering of pro-T cells by PU.1. *Proc Natl Acad Sci U S A* **103**, 11993-11998, doi:0601188103 [pii] 10.1073/pnas.0601188103 (2006).

2 Rosenfeld, N., Young, J. W., Alon, U., Swain, P. S. & Elowitz, M. B. Gene regulation at the single-cell level. *Science* **307**, 1962-1965, doi:307/5717/1962 [pii] 10.1126/science.1106914 (2005).

3 de Celis, J. F. & Bray, S. J. The Abruptex domain of Notch regulates negative interactions between Notch, its ligands and Fringe. *Development* **127**, 1291-1302 (2000).

4 Megason, S. G. & Fraser, S. E. Digitizing life at the level of the cell: high-performance laser-scanning microscopy and image analysis for in toto imaging of development. *Mech Dev* **120**, 1407-1420, doi:S0925477303002120 [pii] (2003).

5 Koster, R. W. & Fraser, S. E. Tracing transgene expression in living zebrafish embryos. *Dev Biol* **233**, 329-346, doi:10.1006/dbio.2001.0242 S0012-1606(01)90242-8 [pii] (2001).

6 Hansson, E. M. *et al.* Recording Notch signaling in real time. *Dev Neurosci* **28**, 118-127, doi:DNE20060281_2118 [pii] 10.1159/000090758 (2006).

7 Weng, A. P. *et al.* Activating mutations of NOTCH1 in human T cell acute lymphoblastic leukemia. *Science* **306**, 269-271, doi:306/5694/269 [pii] 10.1126/science.1102160 (2004).

8 Sheff, M. A. & Thorn, K. S. Optimized cassettes for fluorescent protein tagging in Saccharomyces cerevisiae. *Yeast* **21**, 661-670, doi:10.1002/yea.1130 (2004).

9 Shaner, N. C. *et al.* Improved monomeric red, orange and yellow fluorescent proteins derived from Discosoma sp. red fluorescent protein. *Nat Biotechnol* **22**, 1567-1572, doi:nbt1037 [pii] 10.1038/nbt1037 (2004).

10 Kakidani, H. & Ptashne, M. GAL4 activates gene expression in mammalian cells. *Cell* **52**, 161-167, doi:0092-8674(88)90504-1 [pii] (1988).

11 Nichols, J. T. *et al.* DSL ligand endocytosis physically dissociates Notch1 heterodimers before activating proteolysis can occur. *J Cell Biol* **176**, 445-458, doi:jcb.200609014 [pii] 10.1083/jcb.200609014 (2007).

12 Rothenberg, E. V., Moore, J. E. & Yui, M. A. Launching the T-cell-lineage developmental programme. *Nat Rev Immunol* **8**, 9-21, doi:nri2232 [pii] 10.1038/nri2232 (2008).

13 Gor, V., Bacarian, T., Elowitz, M. & Mjolsness, E. in *Computer Vision and Pattern Recognition (CVPR)* (2005).

Table S3: Simulation Parameters

All simulations (Figs. 3H, 4 B,C,D,G, and S5) were performed using the ode15s ordinary differential equation solver of Matlab. The following equations and parameters were used in the simulations:

Figure	Equations	Parameters	Initial conditions and remarks
3H	Eqs. 8-10,12 in theoretical supplementary	γ = 0.1, γ_S = 0.1, γ_R = 0.1, k_t = 2, k_c = .2, k_{RS} = 1500, β_N = 1, β_D = 0, β_R = 1.8X10^8, p = 2, D_p = {0.063, 0.084, 0.11, 0.15, 0.20, 0.26, 0.35, 0.46, 0.62, 0.82, 1.1, 1.4}	Dimensional units*. D_0 = 200, $N_0 = \frac{\beta_N}{\gamma+\frac{D_0}{k_c}+\frac{D_p}{k_t}}$.
Box, S11	Eqs. 8-10, 12 in theoretical supplementary	γ = 0.1, γ_S = 1.0, D_p=0, k_t = 10, k_c = 1, β_N = 20, β_D = {various from 0 to 40}	Dimensional units*. Plot displays status of cell 1 (left column of equations) with D_2 and N_2 = 0.
4B	Eqs. 21-23 in theoretical supplementary	γ = 0.1, γ_S = 1.0, k_t = 10, k_c = {0.5, 1, 10}, β_N = 20, $\beta_D^{(1)}$ = {various from 0 to 34}, $\beta_D^{(2)}$ = 1.35$\beta_D^{(1)}$	Dimensional units*.
4C	Eqs. 24-27 in theoretical supplementary	γ = 0.1, γ_S = 1.0, γ_R = 0.05, k_t = 5, k_c = .25, k_{RS} = 1500, β_N = 10, β_D^0 = 17.5, β_R = 150, p = 2, n = 1, m = 1, x_0 = 7	Dimensional units*. Use periodic boundary conditions.
4F,S17	Eqs. 50-52 in theoretical supplementary	τ =1 , κ_C ={0.55,0.1,0.05} k_{RS} = 3e5, β_N =200 , β_D = 1000, β_R =3000, m = 1, p = 1	Dimensionless, as described in theoretical supplementary. Periodic boundary conditions. $D(0), N(0), R(0)$ were randomly distributed between 0 and $\beta_D, \beta_N, \beta_R$, respectively.
S8	Eqs. 17-20 in theoretical supplementary	γ = 0.1, γ_S = 0.1, γ_R = 0.1, k_t = 2, k_c = .2, k_{RS} = 1500, β_N = 1, β_D = 0, β_R = 1.8X10^8, p = 2, D_p = {3.16, 4.76, 7.15, 10.8, 16.2, 24.3, 36.6, 55.1, 82.8}	Dimensional units*. D_0 = 200, $N_0 = \frac{\beta_N}{\gamma+\frac{D_0}{k_c}+\frac{D_p}{k_t}}$.
S10A Top Left	blue: Eqs. 24-27 in theoretical supplementary red: Eqs. 32-35 in theoretical supplementary green: Eqs. 36-39 in theoretical supplementary magenta: Eqs. 40-43 in theoretical supplementary	blue: γ = 0.1, γ_S = 1.0, γ_R = 0.05, k_t = 5, k_c = .25, k_{RS} = 1500, β_N = 10, β_D^0 = 17.5, β_R = 75, p = 2, x_0 = 7	Dimensional units*
		red: γ = 0.1, γ_S = 1.0, γ_R = 0.05, k_t = 5, k_b = 1750, β_N = 10, β_D^0 = 17.5, β_R = 75, p = 8, q = 8, x_0 = 7	
		green: : γ = 0.1, γ_S = 1.0, γ_R = 0.05, k_t = 5, k_b = 1750, k_f = 600, β_N = 0.25, β_N' = 19.75, β_D^0 = 17.5, β_R = 75, p = 8, q = 8, n = 2, x_0 = 7	
		magenta : γ = 0.1, γ_S = 1.0, γ_R = 0.05, k_t = 5, k_b = 1750, k_{f2} = 1800, β_N = 10 , β_D^0 = 35, β_R = 75, p = 8, q = 8, m = 2, x_0 = 7	
S10A Top Right	Same as top left	red: same as top left except β_N = 5	Dimensional units*
		green: same as top left except β_N = 0.125, β_N' = 9.875	
		magenta: same as top left except β_N = 5	
S10A Bottom Left	Same as top left	red: same as top left except β_D^0 = 8.75	Dimensional units*
		green: same as top left except β_D^0 = 8.75	
		magenta: same as top left except β_D^0 = 17.5	
S10A Bottom Right	Same as top left	red: same as top left except β_N = 5, β_D^0 = 8.75	Dimensional units*
		green: same as top left except β_N = 0.125, β_N' = 9.875, β_D^0 = 8.75	
		magenta: same as top left except β_N = 5, β_D^0 = 17.5	
S10B	Eqs. 24-27	black: γ = 0.1, γ_S = 1.0, γ_R = 0.05, k_t = 25, k_c = .05, k_{RS} = 1500, β_N = 10, β_D^0 = 15, β_R = 75, p = 1, x_0 = 7	Dimensional units*
		orange: same as black except β_N =5	
		light blue: same as black except β_D^0 = 7.5	
		gray: same as black except β_N =5, β_D^0 = 7.5	
S10C	Eqs. 28-31	γ = 0.1, γ_S = 1.0, γ_R = 0.05, k_t = 5, k_c = .25, k_{RS} = 1500, β_N = 5, β_N^0 = 5, β_D^0 = 17.5, β_R = 75, p = 2, x_0 = 7, nn=1, k_{nn} as indicated in legend.	Dimensional units*
S16A	Eqs: 6-10	γ = 0.1, γ_S = 0.1, γ_R = 0.1, k_t = 2, k_c = .2, k_{RS} = 1500, β_N = 1, β_D = 0, β_R = 1.8X10^8, β_m = {0.1,10}, γ_m = {0.1,10}, p = 2, D_p =1	Dimensional units*
S16B	Eqs: 6-10	γ = 0.1, γ_S = {0.1, 10}, γ_R = 0.1, k_t = 2, k_c = .2, k_{RS} = {1500,1.5}, β_N = 1, β_D = 0, β_R = 1.8X10^8, β_m = 0.1, γ_m = 0.1, p = 2, D_p =1	Dimensional units*
S16B	Eqs: 6-10	γ = 0.1, γ_S = 0.1, γ_R = 0.1, k_t = 2, k_c = .2, k_{RS} = 1500, β_N = 1, β_D = 0, β_R = 1.8X10^8, β_m = 0.1, γ_m = 0.1, p = 2, D_p =1, τ={0,1}	Dimensional units*. Delay introduced in eq. 7 for the translation step. Used dde23 in Matlab.

* Dimensional units: decay rates, γ, γ_S, γ_R are in hours^{-1}, production rates β_N, β_D, $\beta_R$in RFU/hour, affinities k_{RS}, k_b, k_f, k_{f2}in RFU, $k_c$in RFU x hours, x_0 in cell diameters, $D_p$and k_t in effective plate bound concentrations. Here Relative Fluorescent Units [RFU] replace concentrations which are unknown.

Supplementary Material — Theory

Section I: Cells responding to *trans*-Delta (D_{plate}) and *cis*-Delta (D_i)

Model with mutual inactivation of Delta and Notch in *cis*

Let us first consider the case where cells containing Notch (N_i), Delta (D_i), and a Reporter of Notch signaling activity (R_i) are subjected to D_{plate} (D_p). The reactions we consider are the following:

$N_i + D_p \rightleftharpoons [N_i D_p] \rightarrow S_i + D_p$	*trans*–activation, with association/dissociation rates $k_D^{\pm}$ and cleavage rate k_S
$N_i + D_i \rightleftharpoons [N_i D_i] \rightarrow \varnothing$	*cis*–inhibition, with association/dissociation rates $k_C^{\pm}$ and inact./dilution rate γ_{ND}
$S_i \rightarrow R_i$	Signal activation of reporter

The first reaction represents the interaction of Notch with plate-bound Delta to form a complex that can then either dissociate or be cleaved to release the intracellular domain of Notch, denoted S_i. The dynamics of D_p is not relevant for the results presented below, thus we consider D_p not to be consumed in this binding reaction, so that its level is constant. The second reaction describes *cis*-inhibition with mutual inactivation of Notch and Delta. Note that in this Section we ignore the interaction between Delta in the cell and Notch in neighboring cells (*trans*-Notch), which is explicitly accounted for in the model presented in the Box. This interaction will be considered in Section II below. The third reaction represents the combined process in which the Notch intracellular domain translocates into the nucleus, binds with the CSL complex, and induces the expression of the reporter mRNA (m_R). This process is represented below phenomenologically by an increasing Hill function in the reporter production term.

These reactions are translated to the following set of ordinary differential equations:

$$\dot{N}_i = \beta_{\mathrm{N}} - \gamma_{\mathrm{N}} N_i - \left(k_{\mathrm{D}}^{+} N_i D_p - k_{\mathrm{D}}^{-} [N_i D_p]\right) - \left(k_{\mathrm{C}}^{+} N_i D_i - k_{\mathrm{C}}^{-} [N_i D_i]\right) \quad (1)$$

$$\dot{D}_i = \beta_{\mathrm{D}} - \gamma_{\mathrm{D}} D_i - \left(k_{\mathrm{C}}^{+} N_i D_i - k_{\mathrm{C}}^{-} [N_i D_i]\right) \quad (2)$$

$$\dot{[N_i D_p]} = k_{\mathrm{D}}^{+} N_i D_p - k_{\mathrm{D}}^{-} [N_i D_p] - k_{\mathrm{S}} [N_i D_p] \quad (3)$$

$$\dot{[N_i D_i]} = k_{\mathrm{C}}^{+} N_i D_i - k_{\mathrm{C}}^{-} [N_i D_i] - \gamma_{ND} [N_i D_i] \quad (4)$$

$$\dot{S}_i = k_{\mathrm{S}} [N_i D_p] - \gamma_{\mathrm{S}} S_i \quad (5)$$

$$\dot{m}_{\mathrm{R}i} = f_A (S_i; \beta_{\mathrm{m}}, p, k_{\mathrm{RS}}) - \gamma_{\mathrm{m}} m_{\mathrm{R}i} \quad (6)$$

$$\dot{R}_i = \alpha_R m_{\mathrm{R}i} - \gamma_{\mathrm{R}} R_i \quad (7)$$

The function $f_A (S_i; \beta_{\mathrm{m}}, p, k_{\mathrm{RS}})$ is an activating Hill function of the form $\beta_{\mathrm{m}} \frac{S_i^p}{k_{\mathrm{RS}}^p + S_i^p}$. We assume fast cleavage of the Notch-D_{plate} complex, which allows us to apply the quasi-steady-state approximation to its dynamics ($\dot{[N_i D_p]} \approx 0$). Furthermore, we assume that Notch binds to *cis*-Delta irreversibly ($k_{\mathrm{C}}^{-} = 0$), and in that way the dynamics of

Notch does no longer depend on the $[N_iD_i]$ complex. Finally, we consider that the relaxation time of the receptor mRNA is much shorter than the protein relaxation times. With these approximations, the model is reduced to

$$\dot{N}_i = \beta_N - \gamma N_i - N_i \frac{D_p}{k_t} - N_i \frac{D_i}{k_c} \tag{8}$$

$$\dot{D}_i = \beta_D - \gamma D_i - N_i \frac{D_i}{k_c} \tag{9}$$

$$\dot{S}_i = N_i \frac{D_p}{k_t} - \gamma_S S_i \tag{10}$$

$$\dot{R}_i = f_A\left(\frac{1}{\gamma_S} N_i \frac{D_p}{k_t}; \beta_R, p, k_{RS}\right) - \gamma_R R_i \tag{11}$$

where we have defined $\beta_R = \frac{\beta_m \alpha_R}{\gamma_m}$, $k_t^{-1} \equiv \frac{k_D^+ k_S}{k_D^- + k_S}$ and $k_c^{-1} \equiv k_C^+$. We also take the simplifying assumption that $\gamma_N = \gamma_D \equiv \gamma$ (solving with different degradation rates is straightforward). Additionally, and based on the simplifying assumption that the promoter of the reporter R is a far from saturation (i.e., that $k_{RS} \gg \frac{1}{\gamma_S} N_i \frac{D_p}{k_t}$), we approximate its expression as

$$\dot{R}_i = \beta_R \left(\frac{1}{\gamma_S k_{RS}} N_i \frac{D_p}{k_t}\right)^p - \gamma_R R_i \tag{12}$$

We define the total concentration of Delta in the cell as $D_{tot} = D_i + [N_i D_i]$. Using Eqs. (2) and (4) and assuming $\gamma = \gamma_{ND}$, we find that D_{tot} follows a simple linear dynamics:

$$\dot{D}_{tot} = \beta_D - \gamma D_{tot} \tag{13}$$

This result holds even if the Notch-Delta binding is reversible ($k_C^- \neq 0$), provided $\gamma = \gamma_{ND}$. The assumption of equal decay rates for both active Delta and the $[N_iD_i]$ complex is based on the experimental fact that adding Notch to our Delta-expressing cells does not lead to extra decrease of Delta levels beyond dilution. The trivial decay dynamics given by Eq. (13) is observed e.g. in the experiments of Fig. 3C, in which $\beta_D = 0$. Equations (8)–(10) and (12) are the ones used in the simulations shown in Figs. 3H and Box.

Ultrasensitive response of the mutual inactivation switch

Equations (8)–(9) and (12) can be readily solved in the steady state, leading to the following stationary levels of Notch and Delta:

$$N_{st} = \frac{\beta_N - \beta_D}{2g} - \frac{\gamma k_c}{2} + \sqrt{\left(\frac{\beta_N - \beta_D}{2g} - \frac{\gamma k_c}{2}\right)^2 + \frac{k_c \gamma \beta_N}{g}} \tag{14}$$

$$D_{st} = \frac{\beta_D}{\gamma + \frac{N_{st}}{k_c}} \tag{15}$$

where $g = \gamma + D_p/k_t$. This solution is plotted in the Box figure of the main text, for the parameter values given in the Supplementary Table S3. For $\beta_N > \beta_D$ the system reaches a steady state of high Notch and low Delta, in which the cell can send, but not receive, signals. Conversely, when $\beta_D > \beta_N$ the steady state corresponds to high Delta and low Notch, and the cell can receive, but not send, signals. In order to quantify how sensitive the cell is in the region around the switch, we define the sensitivity parameter as the logarithmic derivative of the steady-state signal S_{st} with respect to a control parameter [1], which here we take to be the production rate of Delta, β_D:

$$\xi = \frac{d \log S_{st}}{d \log \beta_D}$$

According to Eq. (10), $S_{\rm st} = D_p N_{\rm st}/\gamma_S k_t$, so that using the result given in (14) at the switch location ($\beta_{\rm D} = \beta_{\rm N}$, where the sensitivity is maximal), and in the limit of large *cis*-inhibition, $\gamma k_c \ll \beta_{\rm N}/(\gamma + D_p/k_t)$, the sensitivity of the switch is approximately [2]

$$\xi \approx \sqrt{\frac{\beta_{\rm N}}{4k_c\gamma(\gamma + D_p/k_t)}} \tag{16}$$

For the parameters used in the Box figure, and given in the Supplementary Table S3, the switch is cleary ultrasensitive, with a sensitivity coefficient $\xi \approx 22.4$. This result does not change qualitatively when including reversibility in the binding of Notch and *cis*-Delta, since in the steady state a nonzero value of $k_{\rm C}^-$ would simply lead to a renormalization of the *cis*-inhibition parameter in the steady-state calculation, equal to $k_c = \frac{\gamma + k_{\rm C}^-}{\gamma k_{\rm C}^+}$.

The sensitivity parameter has been defined above in terms of the signal, S_i, but the experimentally accesible quantity is the reporter's promoter activity, $\dot{R}_i$. The relationship between the reporter sensitivity and the signal sensitivity is given in a straightforward way by

$$\xi_R = \frac{d\log \dot{R}_{\rm st}}{d\log \beta_{\rm D}} = \frac{d\log \dot{R}_{\rm st}}{d\log S_{\rm st}} \frac{d\log S_{\rm st}}{d\log \beta_{\rm D}} \approx p\,\xi\,,$$

where we have assumed that the reporter promoter is far from saturation, as in Eq. (12). Thus the sensitivity measured in our experiments, ξ_R, is a combination of the switch sensitivity, ξ, and the cooperativity p of the reporter promoter.

Another difference between the steady-state calculation presented above and the experimental measurements presented in Fig. 3 is the fact that in the experiments Delta production rate, $\beta_{\rm D}$, is zero, and only the decay of an initial concentration of Delta is observed, as expressed by Eq. (13). Under these conditions, in our experiments we measure the *transient* sensitivity [1] of the reporter's promoter activity as a function of the instantaneous total concentration of Delta, $D_{\rm tot}$. Extensive numerical simulations of our model show that both parameters are similar to each other within 20% in our parameter range.

Alternative model without Delta inactivation by Notch

An alternative model that fails to account for several distinctive features of this system (see text) proposes that the receptor-ligand interaction is catalytic in Delta (in which case Delta is said to be rapidly recycled). The corresponding reactions are the following:

$\mathrm{N}_i + \mathrm{D}_p \rightleftharpoons [\mathrm{N}_i\mathrm{D}_p] \rightarrow \mathrm{D}_p + \mathrm{S}_i$	*trans*–activation, with association/dissociation rates $k_D^{\pm}$ and cleavage rate k_S
$\mathrm{N}_i + \mathrm{D}_i \rightleftharpoons [\mathrm{N}_i\mathrm{D}_i] \rightarrow \mathrm{D}_i$	*cis*–inhibition, with association/dissociation rates $k_C^{\pm}$ and inactivation rate k_E
$\mathrm{S}_i \rightarrow \mathrm{R}_i$	Signal activation of reporter

The *cis*-inhibition reaction now conserves Delta, unlike the mutual-inactivation model. Using the same assumptions made in the preceding case, we obtain the following ordinary differential equations:

$$\dot{N}_i = \beta_{\rm N} - \gamma N_i - N_i\frac{D_p}{k_t} - N_i\frac{D_i}{k_c} \tag{17}$$

$$\dot{D}_i = \beta_{\rm D} - \gamma D_i \tag{18}$$

$$\dot{S}_i = N_i\frac{D_p}{k_t} - \gamma_{\rm S} S_i \tag{19}$$

$$\dot{R}_i = f_A\left(\frac{1}{\gamma_{\rm S}} N_i\frac{D_p}{k_t}; \beta_{\rm R}, p, k_{\rm RS}\right) - \gamma_{\rm R} R_i \tag{20}$$

which are the basis of the data in Fig. S8.

We note that in this case the steady-state solution of Eqs. (17)-(18) leads to the straightforward relation

$$N_{\rm st} = \frac{\gamma\beta_{\rm N}}{1+\frac{D_p}{\gamma k_t}+\frac{\beta_{\rm D}}{k_c}}\,,$$

which shows no sensitivity ($\xi = 1$) with respect to the control parameter $\beta_{\rm D}$.

Effect of finite mRNA and signal lifetimes and reporter expression delay

In the previous paragraphs we have assumed that the lifetimes of the signal, S_i, and of the reporter mRNA, m_{Ri}, are very small in comparison with those of the proteins. We have also considered that the expression of the reporter is instantaneously determined by the level of signal. In order to ascertain that these approximations do not affect the qualitative behavior of our model as described above, we performed simulations of model (1)-(7), maintaining the assumptions of a fast cleavage of the Notch-D_{plate} complex and irreversible binding between Notch and *cis*-Delta. We also added a finite delay τ in the Hill function f_A describing the transcription of the reporter mRNA, Eq. (6), which is now made to depend on the signal S_i at an earlier time τ.

Figure S16 shows the effect of these three factors, namely γ_m, γ_S, and τ, independently of each other. As expected, slower decays of the reporter mRNA and signal (plots A and B) lead to a delay in the turn-on of the reporter. A similar effect is observed in the presence of a time delay in the expression of the reporter with respect to the signal (plot C). In spite of these time shifts, the ultrasensitivity of the switch is not substantially affected, with at most a 30% change in ξ for lifetime variations in the 100× range. We also note that in these simulations the reporter expression is assumed to depend cooperatively on the signal, with a Hill coefficient $p = 2$ that is on the order of the experimentally observed value. Other parameters used in Fig. S16 are given in the Supplementary Table S3.

Section II: Two cells with varying Delta expression

In Fig. 4B of the text we show the amplification of Notch signaling in a cell with some $\beta_{\rm D}^{(1)}$ with a neighbor identical except for a higher Delta production rate $\beta_{\rm D}^{(2)}$ such that $\beta_{\rm D}^{(2)} \gtrsim \beta_{\rm N} \gtrsim \beta_{\rm D}^{(1)}$. The equations used to generate the figure are:

$$\dot{N}_1 = \beta_{\rm N} - \gamma N_1 - N_1\tfrac{D_2}{k_t} - N_1\tfrac{D_1}{k_c} \qquad \dot{N}_2 = \beta_{\rm N} - \gamma N_2 - N_2\tfrac{D_1}{k_t} - N_2\tfrac{D_2}{k_c} \tag{21}$$

$$\dot{D}_1 = \beta_{\rm D}^{(1)} - \gamma D_1 - N_2\tfrac{D_1}{k_t} - N_1\tfrac{D_1}{k_c} \qquad \dot{D}_2 = \beta_{\rm D}^{(2)} - \gamma D_2 - N_1\tfrac{D_2}{k_t} - N_2\tfrac{D_2}{k_c} \tag{22}$$

$$\dot{S}_1 = N_1\tfrac{D_2}{k_t} - \gamma_{\rm S} S_1 \qquad \dot{S}_2 = N_2\tfrac{D_1}{k_t} - \gamma_{\rm S} S_2 \tag{23}$$

Fig. 4B displays the numerical steady-state solution of these equations with parameter values as indicated in the Supplementary Table S3. Note that in Eq. (22) we have assumed that Delta is degraded due to its *trans* interaction with Notch. This is not, however, an essential feature of our model; ultrasensitivity is preserved even when Delta does not degrade in *trans*.

Section III: Spatially-varying Delta expression

Mutual inactivation model

In Figs. 4C,D we consider a field of cells in which Delta production is given by $\beta_{\mathrm{D}}(x) = \beta_{\mathrm{D}}^{0} e^{-|x|/x_0}$ as a function of distance x from a central axis, yielding the axially-symmetric equations:

$$\dot{N}_i = \beta_{\mathrm{N}} - \gamma N_i - N_i \frac{D_i}{k_c} - N_i \frac{\langle D_j \rangle_i}{k_t} \tag{24}$$

$$\dot{D}_i = \beta_{\mathrm{D}}(x) - \gamma D_i - N_i \frac{D_i}{k_c} - \langle N_j \rangle_i \frac{D_i}{k_t} \tag{25}$$

$$\dot{S}_i = N_i \frac{\langle D_j \rangle_i}{k_t} - \gamma_{\mathrm{S}} S_i \approx 0 \quad \Longrightarrow \quad S_i \approx \frac{1}{\gamma_{\mathrm{S}}} N_i \frac{\langle D_j \rangle_i}{k_t} \tag{26}$$

$$\dot{R}_i = f_A(S_i; \beta_{\mathrm{R}}, p, k_{\mathrm{RS}}) - \gamma_{\mathrm{R}} R_i \tag{27}$$

The notation $\langle D_j \rangle_i$ refers to the average over Delta levels of all neighbors j of cell i. In particular, $\langle D_j \rangle_i \equiv \sum_j M_{ij} D_j$ where M is the connectivity matrix of a two-dimensional hexagonal lattice in which

$$M_{ij} = \begin{cases} 1/6 & \text{if } i \text{ and } j \text{ are neighbors} \\ 0 & \text{otherwise} \end{cases}$$

This assumes that Delta and Notch are uniformly distributed over the boundary of the cell. The notation $\langle N_j \rangle_i$ is defined similarly. Note that we now assume that the signal decays sufficiently faster than Notch, Delta and the reporter, which allows us to adiabatically eliminate its dynamics [Eq. (26)]. Figure S10 indicates the ratiometric character of this model by demonstrating that a common rescaling of β_{N} and β_{D} leaves the pattern unchanged.

Band–pass filter model

One could alternatively conceive of a model in which Delta expression still varies as $\beta_{\mathrm{D}}(x)$ above, but instead of mutual inactivation there is a process that restricts expression of the Reporter within a narrow band of Signal values centered about some k_{b}. This band–pass model is governed by the following equations:

$$\dot{N}_i = \beta_{\mathrm{N}} - \gamma N_i \tag{28}$$

$$\dot{D}_i = \beta_{\mathrm{D}}(x) - \gamma D_i \tag{29}$$

$$\dot{S}_i = N_i \frac{\langle D_j \rangle_i}{k_t} - \gamma_{\mathrm{S}} S_i \approx 0 \quad \Longrightarrow \quad S_i \approx \frac{1}{\gamma_{\mathrm{S}}} N_i \frac{\langle D_j \rangle_i}{k_t} \tag{30}$$

$$\dot{R}_i = \beta_{\mathrm{R}} \frac{S_i^p}{k_{\mathrm{b}}^p + S_i^p} \frac{k_{\mathrm{b}}^q}{k_{\mathrm{b}}^q + S_i^q} - \gamma_{\mathrm{R}} R_i \tag{31}$$

Figure S10 shows that this model is not ratiometric.

Band–pass filter model with Signal activating Notch

Adding a proposed mechanism by which Notch signaling induces Notch expression to the band–pass filter model, we have

$$\dot{N}_i = \beta_{\mathrm{N}} + \beta'_{\mathrm{N}} \frac{S_i^n}{k_{\mathrm{f}}^n + S_i^n} - \gamma N_i \tag{32}$$

$$\dot{D}_i = \beta_{\mathrm{D}}(x) - \gamma D_i \tag{33}$$

$$\dot{S}_i = N_i \frac{\langle D_j \rangle_i}{k_t} - \gamma_{\mathrm{S}} S_i \approx 0 \quad \Longrightarrow \quad S_i \approx \frac{1}{\gamma_{\mathrm{S}}} N_i \frac{\langle D_j \rangle_i}{k_t} \tag{34}$$

$$\dot{R}_i = \beta_{\mathrm{R}} \frac{S_i^p}{k_{\mathrm{b}}^p + S_i^p} \frac{k_{\mathrm{b}}^q}{k_{\mathrm{b}}^q + S_i^q} - \gamma_{\mathrm{R}} R_i \tag{35}$$

Figure S10 shows that the addition of the Notch induction term does not generate a ratiometric response.

Band–pass filter model with Signal repressing Delta

Another potential feedback which we can include in the band–pass filter model is one in which Notch signaling represses Delta expression. In this case the model reads

$$\dot{N}_i = \beta_{\mathrm{N}} - \gamma N_i \tag{36}$$

$$\dot{D}_i = \frac{\beta_{\mathrm{D}}(x)}{1 + (S/k_{f2})^m} - \gamma D_i \tag{37}$$

$$\dot{S}_i = N_i \frac{\langle D_j \rangle_i}{k_t} - \gamma_{\mathrm{S}} S_i \approx 0 \quad \Longrightarrow \quad S_i \approx \frac{1}{\gamma_{\mathrm{S}}} N_i \frac{\langle D_j \rangle_i}{k_t} \tag{38}$$

$$\dot{R}_i = \beta_{\mathrm{R}} \frac{S_i^p}{k_{\mathrm{b}}^p + S_i^p} \frac{k_{\mathrm{b}}^q}{k_{\mathrm{b}}^q + S_i^q} - \gamma_{\mathrm{R}} R_i \tag{39}$$

Also for this feedback, Fig. S10 shows that the resulting response is not ratiometric.

Section IV: Lateral inhibition patterning

In order to see the effect of Notch-Delta mutual inactivation on lateral inhibition patterning, let us first consider the classic lateral inhibition model studied by Collier *et al.* [3]:

$\mathrm{N}_i + \mathrm{D}_j \rightleftharpoons [\mathrm{N}_i\mathrm{D}_j] \rightarrow \mathrm{S}_i + \mathrm{N}_i + \mathrm{D}_j$	*trans*–activation, with association/dissociation rates $k_D^{\pm}$ and cleavage rate k_S
$\mathrm{S}_i \rightarrow \mathrm{R}_i$	Signal activation of reporter/repressor as Hill function
$\mathrm{R}_i \dashv \mathrm{D}_i$	Repression of Delta

The *trans*-activation here does not entail the degradation or inactivation of either Notch or Delta. The third reaction introduces feedback of incoming signaling on Delta expression. Applied to a two-dimensional hexagonal lattice of cells (as shown in Fig. 4F), these become the following set of ordinary differential equations:

$$\dot{N}_i = \beta_{\mathrm{N}} - \gamma N_i \tag{40}$$

$$\dot{D}_i = f_R(R_i; \beta_{\mathrm{D}}, m, k_{\mathrm{DR}}) - \gamma D_i \tag{41}$$

$$\dot{S}_i = N_i \frac{\langle D_j \rangle_i}{k_t} - \gamma_{\mathrm{S}} S_i \approx 0 \quad \Longrightarrow \quad S_i \approx \frac{1}{\gamma_{\mathrm{S}}} N_i \frac{\langle D_j \rangle_i}{k_t} \tag{42}$$

$$\dot{R}_i = f_A(S_i; \beta_{\mathrm{R}}, p, k_{\mathrm{RS}}) - \gamma_{\mathrm{R}} R_i \tag{43}$$

The function $f_R\left(R_i;\beta_{\mathrm{D}},m,k_{\mathrm{DR}}\right)$ is a repressive Hill function of the form $\beta_{\mathrm{D}}\frac{k_{\mathrm{DR}}^m}{k_{\mathrm{DR}}^m+R_i^m}$. It is now worth switching to dimensionless units by transforming variables as $t\equiv \mathrm{t}\gamma_{\mathrm{R}}$, $N\equiv\frac{N}{N_0}$, $D\equiv\frac{D}{D_0}$, and $R\equiv\frac{R}{k_{\mathrm{DR}}}$ where $N_0\equiv\frac{\beta_{\mathrm{N}}}{\gamma}$ and $D_0\equiv\frac{\gamma_{\mathrm{S}}k_{RS}}{k_t}\frac{1}{N_0}$ to give

$$\tau\dot{N}_i = 1-N_i \tag{44}$$

$$\tau\dot{D}_i = \beta_D\frac{1}{1+R_i^m}-D_i \tag{45}$$

$$\dot{R}_i = \beta_R\frac{\left(N_i\left\langle D_j\right\rangle_i\right)^p}{1+\left(N_i\left\langle D_j\right\rangle_i\right)^p}-R_i \tag{46}$$

where $\tau\equiv\frac{\gamma_{\mathrm{R}}}{\gamma}$, $\beta_D\equiv\frac{\beta_{\mathrm{D}}}{D_0\gamma}$, and $\beta_R\equiv\frac{\beta_{\mathrm{R}}}{k_{\mathrm{DR}}\gamma_{\mathrm{R}}}$.

These equations can, under certain parameter ranges, generate lateral inhibition patterns as was shown by Collier *et al.* [3]. Recently, Plahte [4] has shown that the product of cooperativities $pm\equiv n$ must exceed 1 for a one-dimensional array of cells. Here we show that for a two-dimensional hexagonal lattice the condition on the product of cooperativities is more stringent, $n>2$.

It is immediately clear that a necessary condition for patterning is the *in*stability of the homogeneous steady state (N^*,D^*,R^*) in which every cell has the same value of N_i, D_i, and R_i. Thus a linear stability analysis about the homogeneous steady state can provide necessary conditions for patterning [4]. The stability analysis requires the computation of the Jacobian at the homogeneous steady state, which is in this case complicated by the large number of variables (three times the number of cells). This is made simpler by an observation originally from Othmer and Scriven [5] that the Jacobian can be expressed as the sum of two tensor products of matrices, one for the internal dynamics and the other for interactions with neighbors: $J=I_k\otimes H+M\otimes B$. The matrix tensor product is defined as $A\otimes B=\begin{pmatrix}a_{11}B & \cdots & a_{1k}B\\ \vdots & \ddots & \vdots\\ a_{k1}B & \cdots & a_{kk}B\end{pmatrix}$. Also, here I_k is the $k\times k$ identity matrix (k is the number of cells involved in the interactions in question), $H_{ij}=\frac{\partial\dot{q}_i}{\partial q_j}$ is the change in production of species i for a change in species j in the same cell, M is the connectivity matrix as defined above, and $B_{ij}=\frac{\partial\dot{q}_i}{\partial\langle q_j\rangle}$ is the change in production of species i for a change in species j in a neighboring cell. N, D, and R correspond to species $i=1,2,3$ respectively. For the model described above, the matrices are:

$$H=\begin{pmatrix}-\frac{1}{\tau} & 0 & 0\\ 0 & -\frac{1}{\tau} & -\frac{D^*}{\tau R^*}mg_0\\ \frac{R^*}{N^*}pf_0 & 0 & -1\end{pmatrix}\ \text{and}\ B=\begin{pmatrix}0 & 0 & 0\\ 0 & 0 & 0\\ 0 & \frac{R^*}{D^*}pf_0 & 0\end{pmatrix} \tag{47}$$

where $g_0\equiv\frac{(R^*)^m}{1+(R^*)^m}$ and $f_0\equiv\frac{1}{1+(N^*D^*)^p}$ are both ≤ 1. Othmer and Scriven [5] proved that the eigenvalues of the overall Jacobian are the eigenvalues of the various matrices $H+q_kB$ where q_k are the eigenvalues of the connectivity matrix M. Thus the eigenvalues λ of the Jacobian are set by the characteristic equation:

$$\begin{vmatrix}-\frac{1}{\tau}-\lambda & 0 & 0\\ 0 & -\frac{1}{\tau}-\lambda & -\frac{D^*}{\tau R^*}mg_0\\ \frac{R^*}{N^*}pf_0 & \frac{R^*}{D^*}pf_0q_k & -1-\lambda\end{vmatrix}=0 \tag{48}$$

which aside from $\lambda=-\frac{1}{\tau}$ happens to be quadratic in λ, meaning that for every q_k there are two eigenvalues of the Jacobian

$$\lambda_\pm=\frac{-\left(1+\frac{1}{\tau}\right)\pm\sqrt{\left(1+\frac{1}{\tau}\right)^2-\frac{4}{\tau}\left(pmg_0f_0q_k+1\right)}}{2} \tag{49}$$

For instability we need only that a single λ have a real part that is positive, which will be so if $pmg_0f_0q_k \leq -1$. An analysis of the matrix M in [5] tells us that $q \geq -0.5$, meaning that $pmg_0f_0 > 2$ and, as $g_0, f_0 \leq 1$, $pm \equiv n > 2$ is a lower bound on the overall cooperativity of the system that must be satisfied for patterning to occur.

cis-Inhibition

To incorporate *cis*-inhibition we add an interaction $\mathrm{N}_i + \mathrm{D}_i \rightleftharpoons [\mathrm{N}_i\mathrm{D}_i] \rightarrow \varnothing$, and modify the *trans*-activation to annihilate Notch and Delta. Here it is more convenient to switch into a different set of dimensionless parameters in which Notch and Delta are normalized by the same quantity: $t \equiv \gamma_R \mathrm{t}$, $N \equiv \frac{N}{N_0}$, $D \equiv \frac{D}{D_0}$, and $R \equiv \frac{R}{R_0}$ where $N_0 = D_0 \equiv \gamma k_t$, and $R_0 \equiv k_{\mathrm{DR}}$. The equations are then

$$\tau \dot{N}_i = \beta_N - N_i - N_i \langle D_j \rangle_i - N_i \frac{D_i}{\kappa_c} \tag{50}$$

$$\tau \dot{D}_i = \beta_D \frac{1}{1 + R_i^m} - D_i - \langle N_j \rangle_i D_i - N_i \frac{D_i}{\kappa_c} \tag{51}$$

$$\dot{R}_i = \beta_R \frac{\left(N_i \langle D_j \rangle_i\right)^p}{k_{RS}^p + \left(N_i \langle D_j \rangle_i\right)^p} - R_i \tag{52}$$

where $\tau \equiv \frac{\gamma_{\mathrm{R}}}{\gamma}$, $\beta_N \equiv \frac{\beta_{\mathrm{N}}}{\gamma N_0}$, $\beta_D \equiv \frac{\beta_{\mathrm{D}}}{\gamma D_0}$, $\beta_R \equiv \frac{\beta_{\mathrm{R}}}{\gamma_{\mathrm{R}} R_0}$, $\kappa_c \equiv \frac{k_c}{k_t}$, and $k_{RS} \equiv \frac{k_{\mathrm{RS}}\gamma_{\mathrm{S}}k_t}{N_0 D_0}$. These were used in Figs. 4F (right panel) and S17, which demonstrate patterning even with $pm \equiv n = 1$.

References

[1] N.E. Buchler and M. Louis, *J. Mol. Biol.* **384**, 1106 (2008).

[2] E. Levine, Z. Zhang, T. Kuhlman, T. Hwa, *PLOS Biol.* **5**(9), e229 (2007).

[3] J.R. Collier, N.A.M. Monk, P.K. Maini, J.H. Lewis, *J. Theor. Biol.* **183**, 429 (1996).

[4] E. Plahte, *J. Math. Biol.* **43**, 411 (2001).

[5] H.G. Othmer, L.E. Scriven, *J. Theor. Biol.* **32**, 507 (1971).